IEEE Access
Multidisciplinary | Rapid Review | Open Access Journal

Received November 20, 2017, accepted December 13, 2017, date of publication December 25, 2017,
date of current version February 14, 2018.

Digital Object Identifier 10.1109/ACCESS.2017.2787055

Performance Analysis of Wireless Energy Harvesting Multihop Cluster-Based Networks Over Nakagami-*m* Fading Channels

NGUYEN TOAN VAN[1], TRI NHU DO[1], (Student Member, IEEE), VO NGUYEN QUOC BAO[2], (Senior Member, IEEE), AND BEONGKU AN[3], (Member, IEEE)

[1]Department of Electronics and Computer Engineering in Graduate School, Hongik University, Sejong City 30016, South Korea
[2]School of Telecommunications, Posts and Telecommunications Institute of Technology, Ho Chi Minh City 710372 , Vietnam
[3]Department of Computer and Information Communications Engineering, Hongik University, Sejong City 30016, South Korea

Corresponding author: Beongku An (beongku@hongik.ac.kr)

The work of N. T. Van, T. N. Do, and B. An was supported in part by the Basic Science Research Program through the National Research Foundation of Korea (NRF), Ministry of Education, under Grant 2016R1D1A1B03934898 and in part by the Leading Human Resource Training Program of Regional Neo Industry through NRF, Ministry of Science, ICT and Future Planning, under Grant 2016H1D5A1910577. The work of V. N. Q. Bao was supported by the Vietnam National Foundation for Science and Technology Development under Grant 102.04-2014.32.

ABSTRACT This paper studies the performance analysis of wireless energy harvesting (EH) cluster-based multi-hop networks, where all communication nodes harvest energy from the radiated signals transmitted by multiple power beacons (PBs) to support the information transmission. To this end, we propose three relay selection schemes. The first scheme tries to select the relay harvesting the largest energy to forward information. The second scheme chooses the relay, providing the best data channel gain from the transmitter to forward information. In the third scheme, two relays in two consecutive clusters will be selected based on the maximum EH link and maximum data link. The destination node is equipped with multiple antennas and applies the maximal ratio combining technique to combine its received signal. The system performances in terms of outage probability of three schemes are evaluated in Nakagami-*m* fading environments and verified by Monte Carlo simulations.

INDEX TERMS Energy harvesting, multihop networks, Nakagami-*m* fading channel, outage probability, power beacon, relay selection, wireless powered transfer.

I. INTRODUCTION

Wireless energy harvesting (EH) has been recently emerging as a promising technique to solve the energy constraint problem of the wireless networks [1]. The communication devices are equipped with the circuits capable of harvesting energy from surrounding natural environment in order to maintain their operation [1], [2]. Since the energy and the information can be simultaneously transmitted and received through the radio frequency (RF) signal, the simultaneous wireless information and power transfer (SWIPT) techniques [3] are interested in the literature. Zhang and Ho [4] designed the practical receiver architectures SWIPT-based for multiple input and multiple output (MIMO) broadcasting system to achieve the maximal information rate and energy transfer.

Cooperative relaying techniques have been recognized as an important technique to extend the coverage and capacity of wireless networks. In [5], the time switching relaying (TSR) and power switching relaying (PSR) architectures for the amplify-and-forward (AF) EH cooperative relaying networks are introduced and the obtained results show that the TSR method outperforms the PSR method in terms of throughput at high transmission rate and low signal-to-noise-ratios. Besides AF relaying strategy, Van *et al.* [6] studied the EH incremental decode-and-forward (DF) cooperative relaying scheme, where the maximal ratio combining (MRC) technique is employed at the destination. The DF cooperative network with relay selection methods is also studied in [7], where the EH cooperative network employing opportunistic relay selection (ORS) provided better performance than its counterpart using partial relay selection (PRS) in terms of outage probability and diversity gain. As an extension of [7], Do *et al.* [8] analyzed a general multiuser multirelay SWIPT cooperative network, where the direct link plus opportunistic relay selection (DOS) and direct link plus partial relay

selection (DPS) are considered with AF and DF strategies. The results reveal that for a given signal-to-noise (SNR), DOS outperforms PRS schemes in terms of outage performance and diversity gain.

For achieving the high energy efficiency and expanding the distance of wireless power transfer in large-scale wireless communication networks, the dedicated power beacons (PBs) based on time switching mechanism are introduced in [9]. In practice, the PB is integrated into the base station (BS) or separated deployment from BS [10]. In [11], the primary network employs multiple primary transmitters (PTs) serving as PBs in order to power the source and the relay in secondary network. The outage probability (OP) and throughput performance of EH cognitive radio network (CRNs) were analyzed and evaluated, and the large system model is considered with the number of PTs increasing to infinity. In [12], the multiple PBs are randomly deployed as the base stations in the existing cellular network architectures for recharging mobiles and wireless sensor devices. The tradeoffs between the related system parameters including the PB/mobile transmission power and PB/base station densities for different network settings and mobiles having small/large capacity power storage are also studied. Unlike the SWIPT system in prior works, in the wireless-powered communication networks (WPCN), the harvest-then-transmit protocol was proposed in [13] in which the multiple users first harvest energy from hybrid access-point (H-AP) in the downlink and then use this harvested energy to transmit information back to the H-AP in the uplink phase based on time division multiple access (TDMA). This work focused on the optimal time allocation to maximize the sum-throughput. With respect to WPCN networks, Chen *et al.* [14] studied the system, where the source and the relay use harvest-then-cooperative protocol for data transmission. The obtained results provide that the harvest-then-cooperative protocol outperforms the harvest-then-transmit protocol in all channel settings. The approximate expression of average throughput over Rayleigh fading channels is derived.

These research works assume that the cooperative relay networks operate with single antenna modes or experience Rayleigh fading channels. Over Nakagami-*m* fading channel, the dual hop cooperative DF relaying system employing relay selection technique is introduced in [15] and the dual hop AF relaying network exploiting multi-antennas at the relay is studied in [16]. The obtained results indicate that the shape parameter m, the number of transmit and receive antennas greatly affect on the system diversity. For the EH cooperative networks, Anh *et al.* [17] studied the DF EH network, where the source and the destination are equipped with multi-antennas employing transmit antenna selection (TAS) and MRC techniques, respectively. The distribution PBs assisted EH wireless systems over Nakagami-*m* fading channels is proposed in [18] and the closed-form expression of the throughput in high SNR is also obtained.

Multi-hop cooperative relaying have recently received considerable attention by many researchers to extend the radio coverage and improve network performance, (see, e.g., [19]–[22]). In multi-hop networks, the transmitter consumes less energy for data transmission compared to direct communication. Thus, it is realized in many practical applications, e.g., wireless sensor networks, cellular networks, Internet of Things (IoT), vehicle or personnel tracking and roadside facilities [19]. In particular, Duy and Kong [20] presented the cluster-based multi-hop networks based on various relay selection schemes, where the relay selection method applied for each dual-hop provided better performance than the relay selection applied for single hop transmission. To provide the new insight into the design and optimization of multi-hop network, Bao and Duong [21] studied a cognitive multi-hop networks under interference constraints, where the system outage performance is significantly affected by several factors, such as the number of hops, the secondary users (SUs) and the primary users (PUs). As an extension of [21], Bao *et al.* [22] studied the cognitive multi-hop DF network with imperfect channel state information (CSI) of the interference links in terms of OP, BER and ergodic capacity. Sang and Kong [23] compared the maximum data link based relay selection (MaDS) and minimum relay-eavesdropping link based relay selection (MiES) in the multi-hop cooperative networks. The numerical results show that MaDS outperforms MiES schemes in terms of secrecy performance for all channel settings. For underlay cognitive AF multi-hop relaying networks, Al-Qahtani *et al.* [24] studied the generalized MIMO model using TAS/MRC per hop in secondary network. The exact and asymptotic expressions for outage performance under various interference constraints are obtained and the impacts of PUs number, antennas size of SUs, number of hops and interference outage constrains are also evaluated. However, the above mentioned works just considered the multi-hop cooperative networks without taking the energy harvesting into account.

Considering large-scale multi-hop networks, when a sensor node runs out of energy, which critically affects the reliability and radio coverage of wireless networks. This situation arising a serious question in practice for communication network is how to deal with the energy constrained of sensor nodes. The dedicated power beacons are designed to solve this problem since all communication nodes can scavenge energy from PBs and use this harvested energy for subsequent information transmission. Moreover, instead of supplying power for each node in such a large-scale network, the power beacon is able to ubiquitously radiate the energy to all sensor nodes without human interaction. Therefore, this is an effective solution to prolong wireless device battery life time and improve network energy efficiency. Very recently, Xu *et al.* [25] proposed undelay multi-hop cognitive relay networks where SUs can harvest the energy from PB to support the data transmission. The authors also considered the power optimization issue to improve the energy efficiency and minimize the system OP. A novel multi-hop relaying network is proposed in [26], where the source and the relays harvest energy from external co-channel interferences (CCIs)

to support the data transmission in Nakagami-m fading environments. The analysis results reveal that the system OP and the largest number of hops mainly depend on the quality of desired channels regardless of the CCIs.

However, the last two papers above only considered the single cooperating relay in multi-hop networks. In real scenarios, if an arbitrarily intermediate relay is out of order due to the adversely affected of environment, the network will interrupt. Therefore, employing cluster relays will stabilize the system operation as well as maintain the Quality of Services (QoS) of network. Moreover, applying the relay selection on multi-hop cluster system will enhance the reliability of transmit data and increase the diversity transmission between two adjacent clusters of networks.

This paper studies the effects of relay selection strategies considering generally wireless powered multi-hop cluster-based relay network with multiple power beacons, multiple antennas at destination. Three relay selection approaches are considered. The first scheme, named maximum energy based relay selection (MES), where the selected relay in the desired cluster harvesting the largest energy will be the forwarder in the next hop. The second scheme, named maximum data channel based relay selection (MDS), where the selected relay in the desired cluster providing the best data channel gain from the transmitter will be the forwarder. The third scheme, named maximum energy harvesting and data channels based relay selection (MEDS), where two relays in two consecutive clusters will be selected based on the maximum harvesting energy in the EH phase and maximum data channel gain in the information transmission phase. In addition, we also provide the random relay selection (RRS) scheme as a baseline to demonstrate the merit of our proposed schemes. The obtained results present that MEDS scheme outperforms MDS scheme, which, in turns, outperforms MES scheme. Moreover, the performances of each scheme can be improved by increasing the number of PBs, number of relays in each cluster and number of antennas at the destination. In addition, the optimal time switching ratio and the number of hops are extensively studied. Motivated by the aforementioned works, the main contribution of this paper are summarized as follows:

- We propose three relay selection schemes in multi-hop cooperative networks. Specifically, we introduce the new relay selection method applying for each dual hop to improve communication reliability and system diversity transmission.
- We derive new closed-form expressions of the system outage probability (OP) for MES, MDS and MEDS schemes over Nakagami-m fading channels. The derived analytical results are verified by Monte-Carlo simulation to confirm our correctness.
- We show that for the same channel settings, the MEDS scheme outperforms the MDS scheme, which, in turns, outperforms MES scheme. Moreover, the obtained results reveal that the outage performances of all schemes considerably depend on the number of relays in each cluster, the number of antennas at destination, the number of PBs as well as the position of PBs. Moreover, the system performance can be greatly improved by appropriately designing the time switching ratio for energy harvesting phase and suitably selecting the number of hops for data transmission phase.

The rest of the paper is arranged as follows. Section II introduces the system model and the operated descriptions of the RRS, MES, MDS and MEDS schemes. Section III presents the developed analysis in terms of the OP for the considered schemes. Section IV presents the numerical results based on the derived analytical results. Monte Carlo simulations are shown to corroborate the proposed analysis. Finally, Section V concludes the paper.

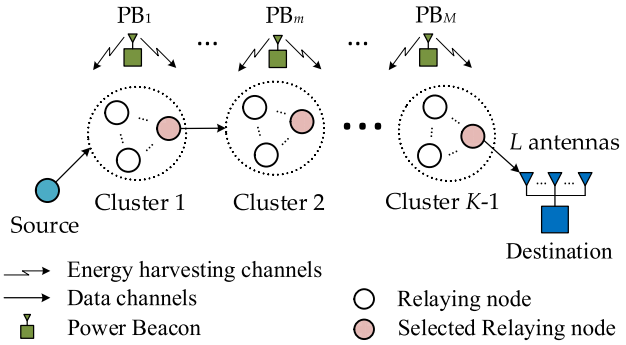

FIGURE 1. Schematic illustration of the wireless powered multi-hop cluster-based network.

II. SYSTEM MODEL AND RELAY SELECTION SCHEMES

A. SYSTEM MODEL

As shown in Fig. 1, we consider the system model of a wireless energy harvesting multi-hop cluster-based relay network, where the source (S) transmits its data to the destination (D) via multiple DF relays locating in $K-1$ intermediate clusters, with $K > 1$. Considering a practical wireless sensor multi-hop network, all nodes have no extra embedded energy supply; hence, they need to harvest energy from multiple power beacons, denoted by $\mathsf{PB}_1, \ldots, \mathsf{PB}_M$, for their cooperative data transmission. We also assume that the source node and the relay nodes are equipped with a single antenna and operate on a half-duplex mode, while the destination, e.g., base station or sink node, is equipped with L antennas and employs the MRC technique to combine multiple copies of the received signals.

A list of main mathematical notations used in this paper is given in Table 1. Moreover, all channels are subject to quasi-static independent identically distributed (i.i.d.) Nakagami-m fading channels and the perfect knowledge of channel state information (CSI) is available at each receiver node. Thus, the channel gain, $|g_{k-1,m,i}|^2$ and $|h_{k,i,j}|^2$, have i.i.d. Nakagami-m distribution with parameter as $\Omega_{k-1} = l_{l-1}^{\beta}$, $\lambda_k = d_k^{\beta}$ and the fading severity m_1 and m_2, respectively. And the average channel gain can be expressed, respectively,

TABLE 1. Summary of main notations.

Notation	Definition
M	The number of power beacons.
L	The number of antennas at D.
P	The transmit power of each power beacon.
N_u	The number of relays in the uth cluster, $u \in \{1, \ldots, K-1\}$ and $N_u \geq 1$.
$\mathsf{R}_{u,v}$	The vth relay in the uth cluster, $v \in \{1, \ldots, N_u\}$.
l_{k-1}	The distance (in meter) between PB_m and $\mathsf{R}_{k-1,i}$, with $i \in \{1, \ldots, N_{k-1}\}$.
d_k	The distance (in meter) between $\mathsf{R}_{k-1,i}$ and $\mathsf{R}_{k,j}$, with $j \in \{1, \ldots, N_k\}$, $\mathsf{R}_0 \equiv \mathsf{S}$ and $\mathsf{R}_K \equiv \mathsf{D}$.
$g_{k-1,m,i}$	The channel coefficient of link $\mathsf{PB}_m \to \mathsf{R}_{k-1,i}$.
$h_{k,i,j}$	The channel coefficient of link $\mathsf{R}_{k-1,i} \to \mathsf{R}_{k,j}$.
$\lvert g_{k-1,m,i}\rvert^2$	The channel gain of link $\mathsf{PB}_m \to \mathsf{R}_{k-1,i}$.
$\lvert h_{k,i,j}\rvert^2$	The channel gain of link $\mathsf{R}_{k-1,i} \to \mathsf{R}_{k,j}$.
Ω_{k-1}, λ_k	Parameters of i.i.d. Nakagami-m distributions.
α	The time switching ratio.
η	The energy conversion efficiency.
β	The pathloss exponent.
m_1, m_2	Nakagami-m fading parameter.
d_0	The reference distance.
$\mathcal{L}$	The measured pathloss at d_0.
σ^2	Noise power level.
$\mathbb{P}_{out}^{\mathcal{S}}$	The outage probability of scheme $\mathcal{S}$.

as $E\left\{|g_{k-1,m,i}|^2\right\} = \frac{\mathcal{L}}{(l_{k-1}/d_0)^\beta}$ and $E\left\{|h_{k,i,j}|^2\right\} = \frac{\mathcal{L}}{(d_k/d_0)^\beta}$. In addition, we use the notation $|h_{\mathsf{D},l}|^2$ instead of $|h_{K,i,l}|^2$ in some cases.

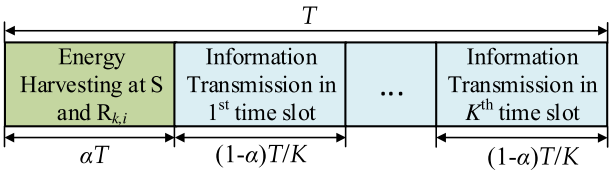

FIGURE 2. The transmission block structure of proposed scheme for energy harvesting and information processing.

B. ENERGY HARVESTING AND INFORMATION TRANSMISSION PROCESSES

The transmission block structure of the proposed system employing time switching architecture [5] is depicted in Fig. 2. The communication between the source node and the destination node in each data frame is carried out in two consecutive phases for energy harvesting and information transmission, respectively. In the EH phase, all relays simultaneously harvest energy from M PBs, while operation of the system in the transmission information phase is split into K orthogonal sub-time slots. For each transmission block T and time switching ratio α_k, the duration of $\alpha_k T$ is used for EH phase while the remaining time, i.e., $(1-\alpha_k)T/K$, is used for the data transmission for each hop. It is reasonable to assume that the harvested energy at each node stores in a super capacitor, then fully consumes to transmit the data signal to next node [3], [5], [7]. Furthermore, all communication nodes are similarly structured; hence, the time switching ratio of them α_k is constant, i.e. $\alpha_k = \alpha$. In addition, the power beacons have the same structure, thus they radiate the same transmit power level, i.e., $\mathrm{P}_k = \mathrm{P}$. The energy harvested at $\mathsf{R}_{k-1,i}$ from M PBs can be given as [5]

$$\mathrm{E}_{k-1} = \sum_{m=1}^{M} \eta\alpha T \mathrm{P}|g_{k-1,m,i}|^2, \tag{1}$$

where η with $\eta \in (0, 1)$ denotes the energy conversion efficiency. Therefore, the average transmit power of $\mathsf{R}_{k-1,i}$ can be expressed as

$$\begin{aligned}\mathrm{P}_{k-1} &= \frac{\mathrm{E}_{k-1}}{(1-\alpha)T/K} \\ &= \sum_{m=1}^{M} \kappa \mathrm{P}|g_{k-1,m,i}|^2,\end{aligned} \tag{2}$$

where κ is defined as $\kappa = K\eta\alpha/(1-\alpha)$.

In the kth hop relaying network, the relay node $\mathsf{R}_{k-1,i}$ forward the re-encoded signal to the next cluster or to the destination. Thus, the received signal at $\mathsf{R}_{k,j}$ can be expressed as

$$y_k = \sum_{m=1}^{M} \sqrt{\mathrm{P}} g_{k,m,j} e_m + \sqrt{\mathrm{P}_{k-1}} h_{k,i,j} x_{k-1} + n_k, \tag{3}$$

where $n_k \sim \mathcal{CN}(0, \sigma_k^2)$, herein $\mathcal{CN}(0, \sigma_k^2)$ is the circular symmetric complex Gaussian variable with zero-mean and variance σ_k^2. Without loss of generality, we assume that each node has the same noise power level, i.e., $\sigma_k^2 = \sigma^2$. And e_m and x_{k-1} are the transmit signal from PB_m and $\mathsf{R}_{k-1,i}$, respectively, wherein $\mathbb{E}[|e_m|^2] = 1$ and $\mathbb{E}[|x_{k-1}|^2] = 1$ with $\mathbb{E}[.]$ being the expectation operator. Two signals e_m and x_{k-1} are not correlated, therefore, e_m is transformed to energy by internal RF converted circuit while x_{k-1} is decoded and forwarded by $\mathsf{R}_{k,j}$.

Next, the instantaneous SNR at $\mathsf{R}_{k,j}$ is calculated as

$$\begin{aligned}\gamma_{k,i,j} &= \frac{\mathrm{P}_{k-1}|h_{k,i,j}|^2}{\sigma^2} \\ &= \sum_{m=1}^{M} \kappa\bar{\gamma}|g_{k-1,m,i}|^2|h_{k,i,j}|^2,\end{aligned} \tag{4}$$

where $\bar{\gamma} = \mathrm{P}/\sigma^2$ denotes the average transmit signal-to-noise ratio (SNR).

At the destination, the relay in cluster $K-1$ use the harvested energy from M PBs to forward the re-encoded signal to the destination. Moreover, D is equipped with L antennas and using MRC technique, the received signal can be expressed as

$$y_{\mathsf{D}} = \sqrt{P_{K-1}} \sum_{l=1}^{L} h_{\mathsf{D},l} x_{K-1} + n_{\mathsf{D}}, \tag{5}$$

where $l \in \{1, \ldots, L\}$.

The instantaneous SNR at the destination node can be formulated as

$$\begin{aligned}\gamma_{\mathsf{D}} &= \frac{P_{K-1}\sum_{l=1}^{L}|h_{\mathsf{D},l}|^2}{\sigma^2} \\ &= \sum_{m=1}^{M} \kappa\bar{\gamma}|g_{K-1,m,i}|^2 \sum_{l=1}^{L}|h_{\mathsf{D},l}|^2.\end{aligned} \tag{6}$$

In the next sub-section, the RRS, MES, MDS and MEDS schemes will be mathematically described in details.

C. RELAY SELECTION SCHEMES

1) SELECTION METHOD OF RRS SCHEME

In this protocol, a randomly selected relay in each cluster will be the forwarder in the next hop. Therefore, the instantaneous SNR for $K-1$ hop transmission is calculated as

$$\gamma_{k,b,j}^{\mathrm{RRS}} = \sum_{m=1}^{M} \kappa\bar{\gamma}|g_{k-1,m,b}|^2|h_{k,b,j}|^2. \quad (7)$$

The instantaneous SNR for the last hop is expressed as

$$\gamma_{\mathsf{D}}^{\mathrm{RRS}} = \sum_{m=1}^{M} \kappa\bar{\gamma}|g_{K-1,m,b}|^2 \sum_{l=1}^{L}|h_{\mathsf{D},l}|^2. \quad (8)$$

2) SELECTION METHOD OF MES SCHEME

In this protocol, a selected relay in each cluster harvesting the largest energy from multiple PBs in the EH phase will be the forwarder in the next hop. The flow chart of MES scheme is shown in Fig. 3. The best relay, $\mathsf{R}_{k,b}$, is selected in cluster k by the following strategy

$$\mathsf{R}_{k,b} = \arg\max_{i=1,\ldots,N_k} \sum_{m=1}^{M} \eta\alpha T\mathrm{P}|g_{k,m,i}|^2. \quad (9)$$

The instantaneous SNR at relay $\mathsf{R}_{k+1,j}$ is calculated as

$$\gamma_{k+1,b,j}^{\mathrm{MES}} = \max_{i=1,\ldots,N_k} \sum_{m=1}^{M} \kappa\bar{\gamma}|g_{k,m,i}|^2|h_{k+1,b,j}|^2. \quad (10)$$

In the last hop, the relay in the cluster $K-1$ harvesting the largest energy will forward the information to the destination node in the Kth time slot. The instantaneous SNR at D can be formulated as

$$\gamma_{\mathsf{D}}^{\mathrm{MES}} = \max_{i=1,\ldots,N_{K-1}} \sum_{m=1}^{M} \kappa\bar{\gamma}|g_{K-1,m,i}|^2 \sum_{l=1}^{L}|h_{\mathsf{D},l}|^2. \quad (11)$$

3) SELECTION METHOD OF MDS SCHEME

In this protocol, a selected relay in each cluster providing the largest data channel gain to the transmitter among available ones will be the forwarder in the next hop. The flow chart of MDS scheme is also shown in Fig. 3. Assuming that the best relay at the cluster $k-1$ is $\mathsf{R}_{k-1,b}$; thus, the best relay at the cluster k is chosen by the following strategy

$$\mathsf{R}_{k,b} = \arg\max_{j=1,\ldots,N_k} \sum_{m=1}^{M} \kappa\bar{\gamma}|g_{k-1,m,b}|^2|h_{k,b,j}|^2. \quad (12)$$

The instantaneous SNR obtained for kth hop transmission is calculated by

$$\gamma_{k,b,j}^{\mathrm{MDS}} = \max_{j=1,\ldots,N_k} \sum_{m=1}^{M} \kappa\bar{\gamma}|g_{k-1,m,b}|^2|h_{k,b,j}|^2. \quad (13)$$

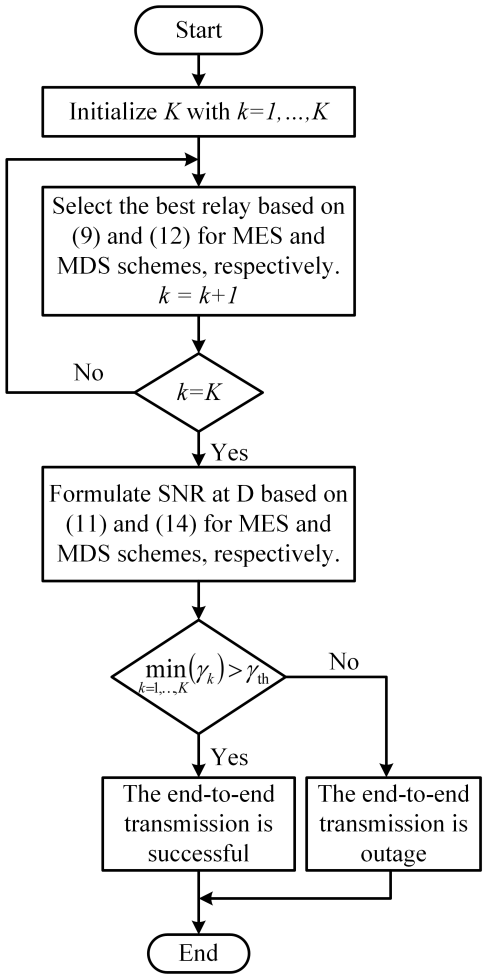

FIGURE 3. The flow chart for the data transmission of MES and MDS schemes.

In the last hop, the selected relay $\mathsf{R}_{K-1,b}$ will forward the re-encoded signal to the destination; hence, the instantaneous SNR at D can be formulated as

$$\gamma_{\mathsf{D}}^{\mathrm{MDS}} = \sum_{m=1}^{M} \kappa\bar{\gamma}|g_{K-1,m,b}|^2 \sum_{l=1}^{L}|h_{\mathsf{D},l}|^2. \quad (14)$$

4) SELECTION METHOD OF MEDS SCHEME

For the purpose of maximizing the SNR of two consecutive hops, a pair of optimal relay in two adjacent clusters will be selected for data transmission. Considering any two consecutive hop transmission including three clusters, the relay in the first and in the third clusters harvesting the largest energy will be selected for data transmission. Then the opportunistic relay selection method [7] is applied to choose the best relay in the second cluster that maximizes the SNR between the first and the third selected relay. It is worth noting that the third selected relay is chosen for the next dual hop transmission. In this scheme, we consider two cases of cluster number including even (Case 1) and odd (Case 2). The flow charts of MEDS scheme for Case 1 and Case 2 are shown in Fig. 4

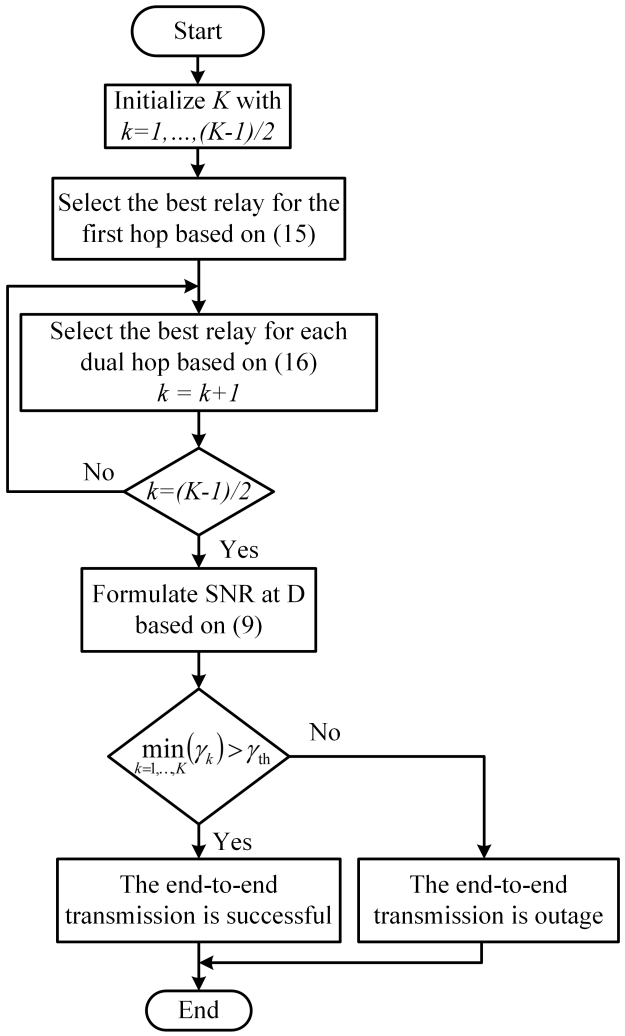

FIGURE 4. The flow chart for the data transmission of MEDS scheme in Case 1.

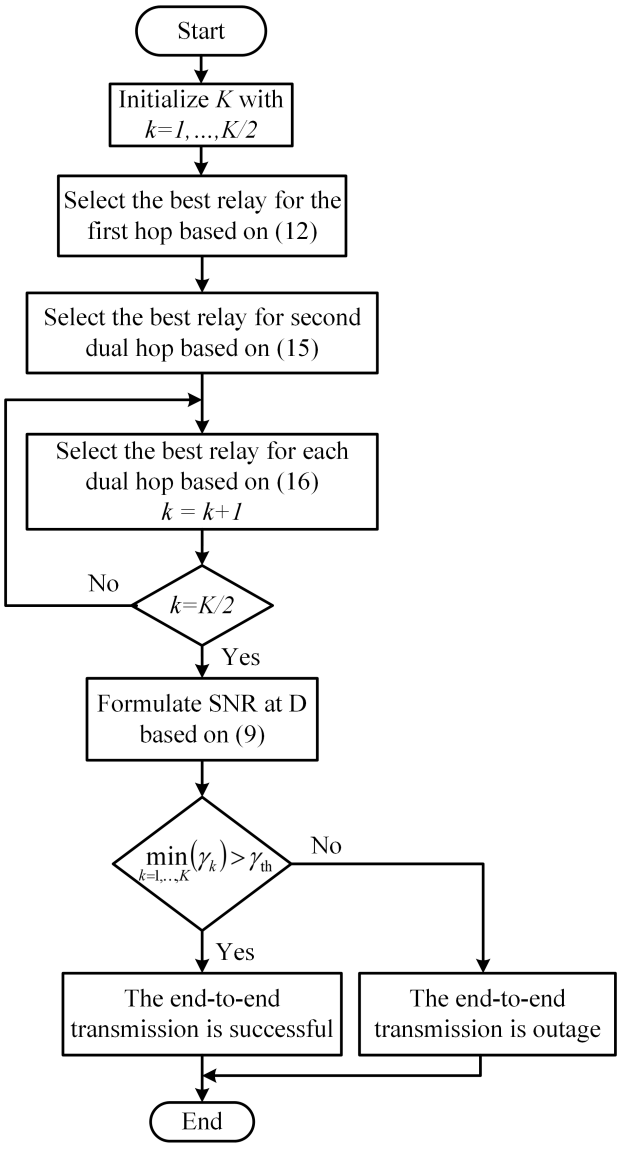

FIGURE 5. The flow chart for the data transmission of MEDS scheme in Case 2.

and Fig. 5, respectively. Two case of the number of cluster are considered as follows:

Case 1: The number of clusters is even

In this case, the relay in the even cluster harvesting the largest energy will be selected before the data transmission process. Considering the first dual hop, the best relay at cluster 1 will be selected as follows:

$$\mathsf{R}_{1,b} = \arg \max_{j=1,\ldots,N_1} \min \times \left\{ \sum_{m=1}^{M} \kappa \bar{\gamma} |g_{0,m,1}|^2 |h_{1,i,j}|^2, \sum_{m=1}^{M} \kappa \bar{\gamma} |g_{1,m,j}|^2 |h_{2,j,b}|^2 \right\}. \quad (15)$$

Next, we assume that the selected relay at cluster $2k$ is $\mathsf{R}_{2k,b}$ with $k \in \{2, \ldots, (K-1)/2\}$ and $(K-1)$ being the number of clusters, then the best relay at clusters $(2k-2)$ and $(2k-1)$ can be selected by the strategy (16), given at the top of the next page.

The instantaneous SNRs for the first dual hop and for kth dual hop transmission are also calculated as (17) and (18), respectively, shown at the top of the next page.

Considering the last hop, the best relay $\mathsf{R}_{K-1,b}$ in cluster $K-1$ is selected based on the strategy (9) in MES scheme to forward the re-encoded signal to the destination node. The MRC technique is employed at D, thus the instantaneous SNR can be formulated as

$$\gamma_{\mathsf{D}}^{\mathrm{MEDS}} = \max_{j=1,\ldots,N_{K-1}} \sum_{m=1}^{M} \kappa \bar{\gamma} |g_{K-1,m,j}|^2 \sum_{l=1}^{L} |h_{\mathsf{D},l}|^2. \quad (19)$$

Case 2: The number of clusters is odd

In this case, the relay in the odd cluster having the largest energy will be selected before the data transmission process. Since the number of hop is even, cluster 1 will select the best relay based on the strategy (12) in MDS scheme for the first single hop transmission, then the cluster 2 selects the best relay based on the strategy (15) for the second dual hop transmission. Subsequent to that, the strategy as in (16) will be

$$(\mathsf{R}_{2k-2,b}, \mathsf{R}_{2k-1,b}) = \arg \max_{j=1,\ldots,N_{2k-1}} \min \left\{ \max_{i=1,\ldots,N_{2k-2}} \sum_{m=1}^{M} \kappa\bar{\gamma}|g_{2k-2,m,i}|^2|h_{2k-1,i,j}|^2, \sum_{m=1}^{M} \kappa\bar{\gamma}|g_{2k-1,m,j}|^2|h_{2k,j,b}|^2 \right\}. \quad (16)$$

$$\gamma_{1,j,b}^{\mathrm{MEDS}} = \max_{j=1,\ldots,N_1} \min \left\{ \sum_{m=1}^{M} \kappa\bar{\gamma}|g_{0,m,1}|^2|h_{1,i,j}|^2, \sum_{m=1}^{M} \kappa\bar{\gamma}|g_{1,m,j}|^2|h_{2,j,b}|^2 \right\}. \quad (17)$$

$$\gamma_{k,j,b}^{\mathrm{MEDS}} = \max_{j=1,\ldots,N_{2k-1}} \min \left\{ \max_{i=1,\ldots,N_{2k-2}} \sum_{m=1}^{M} \kappa\bar{\gamma}|g_{2k-2,m,i}|^2|h_{2k-1,i,j}|^2, \sum_{m=1}^{M} \kappa\bar{\gamma}|g_{2k-1,m,j}|^2|h_{2k,j,b}|^2 \right\}. \quad (18)$$

applied for the next $(K-3)/2$ dual hop transmission. Finally, the best relay, $\mathsf{R}_{K-1,b}$, is selected similarly to Case 1 for the last hop transmission.

III. OUTAGE PERFORMANCE ANALYSIS

In this section, the closed-form expressions of outage probability for the proposed schemes will be provided. The system outage probability can be expressed as

$$\mathbb{P}_{out}^{\mathcal{S}} = \Pr\left[\frac{1-\alpha}{K}\log_2\left(1+\min_{k=1,\ldots,K}\gamma_k^{\mathcal{S}}\right) < \mathcal{R}_{\mathrm{th}}\right], \quad (20)$$

where $\mathcal{S} \in \{\mathrm{RRS}, \mathrm{MES}, \mathrm{MDS}, \mathrm{MEDS}\}$ and $\mathcal{R}_{\mathrm{th}}$ bits/s/Hz is the target data rate. The fraction time of $(1-\alpha)/K$ is accounted for information transmission phase splitting in K orthogonal sub-time slots.

For the sake of simplicity, in the sequel of the paper, $\psi_E(n, \Omega_k, N_k)$ and $\psi_D(n, \lambda_k, N_k)$ denote the multinomial coefficients which are defined in (31) and (50), respectively. Moreover, χ_k and Θ_{k-1} are defined in (38) and (52), respectively. We also assume that m_1 and m_2 are integer numbers. In addition, let $\Pi_k = (m_1\Omega_{k-1}m_2\lambda_k\gamma_{\mathrm{th}})/\kappa$.

A. RRS SCHEME

Theorem 1: The exact closed-form expression of the outage probability for the RRS protocol over Nakagami-m fading channels is given as (21), shown at the top of the next page, where $\gamma_{\mathrm{th}} = 2^{\frac{K\mathcal{R}_{\mathrm{th}}}{1-\alpha}} - 1$ and $\mathbb{K}_\nu(.)$ is the modified Bessel function of the second kind with order ν [27].

Proof: The proof is given in Appendix. ■

B. MES SCHEME

Theorem 2: The exact closed-form expression of the outage probability for the MES scheme over Nakagami-m fading channels is shown in (22), given at the top of the next page.

Proof: In MES scheme, the relay selection method is applied for $(K-1)$ clusters and be excepted for the source node and the destination node. Therefore, we consider the data transmission process in the first hop, $(K-2)$ hop and the last hop. The OP of MES scheme is given as follows:

$$\mathbb{P}_{out}^{\mathrm{MES}} = 1 - \left[1 - F_{\gamma_{1,b,j}^{\mathrm{MES}}}(\gamma_{\mathrm{th}})\right]\left[1 - F_{\gamma_{\mathsf{D}}^{\mathrm{MES}}}(\gamma_{\mathrm{th}})\right] \times \prod_{k=1}^{K-2}\left[1 - F_{\gamma_{k+1,b,j}^{\mathrm{MES}}}(\gamma_{\mathrm{th}})\right], \quad (23)$$

where $F_{\gamma_{1,b,j}^{\mathrm{MES}}}(.)$, $F_{\gamma_{k+1,b,j}^{\mathrm{MES}}}(.)$ and $F_{\gamma_{\mathsf{D}}^{\mathrm{MES}}}(.)$ are the CDF of $\gamma_{1,b,j}^{\mathrm{MES}}$, $\gamma_{k+1,b,j}^{\mathrm{MES}}$ and $\gamma_{\mathsf{D}}^{\mathrm{MES}}$, respectively.

Invoking the Theorem 1, we firstly obtain the CDF of $\gamma_{1,b,j}^{\mathrm{MES}}$ as follows:

$$F_{\gamma_{1,b,j}^{\mathrm{MES}}}(\gamma_{\mathrm{th}}) = 1 - 2\sum_{t=0}^{m_1M-1}\frac{1}{t!\Gamma(m_2)} \times \left(\frac{\Pi_1}{\bar{\gamma}}\right)^{\frac{m_2+t}{2}} \mathbb{K}_{t-m_2}\left(2\sqrt{\frac{\Pi_1}{\bar{\gamma}}}\right). \quad (24)$$

Considering $\gamma_{k+1,b,j}^{\mathrm{MES}}$ in (7), let $X_b = \max_{i=1,\ldots,N_k}\sum_{m=1}^{M}|g_{k,m,i}|^2$ and $Y_j = |h_{k+1,b,j}|^2$. The CDF of $\gamma_{k+1,b,j}^{\mathrm{MES}}$ can be calculated as

$$F_{\gamma_{k+1,b,j}^{\mathrm{MES}}}(\gamma_{\mathrm{th}}) = \int_0^{+\infty} F_{X_b}\left(\frac{\gamma_{\mathrm{th}}}{\kappa\bar{\gamma}x}\right) f_{Y_j}(x)dx. \quad (25)$$

Recalling that X_b is the maximum of N_k i.i.d. gamma distributed random variables (RVs), thus the CDF of X_b can be calculated as

$$F_{X_b}(x) = \left[\frac{\gamma(m_1M, m_1\Omega_k x)}{\Gamma(m_1M)}\right]^{N_k}, \quad (26)$$

where $\gamma(a,z) = \int_0^z t^{a-1}e^{-t}dt$ denotes the incomplete Gamma function [28, eq. (6.5.2)].

Making use of [27, eq. (8.351.2)], i.e.,

$$\gamma(m_1M, m_1\Omega_k x) = (m_1\Omega_k x)^{m_1M}\frac{\exp(-m_1\Omega_k x)}{m_1M} \times {}_1F_1(1, m_1M+1; m_1\Omega_k x) \quad (27)$$

and then utilizing the generalized hypergeometric series [27, eq. (9.14.1)], i.e.,

$${}_1F_1(1, m_1M+1; m_1\Omega_k x) = \sum_{n=0}^{\infty}(m_1\Omega_k x)^n\frac{m_1M\Gamma(m_1M)}{\Gamma(m_1M+1+n)}, \quad (28)$$

the CDF of X_b can be rewritten as follows:

$$F_{X_b}(x) = (m_1\Omega_k x)^{m_1}N_kM\exp(-m_1\Omega_k N_k x) \times \left[\sum_{n=0}^{\infty}\frac{(m_1\Omega_k x)^n}{\Gamma(m_1M+1+n)}\right]^{N_k}. \quad (29)$$

$$\mathbb{P}_{out}^{\text{RRS}} = 1 - \prod_{k=1}^{K-1} \sum_{t=0}^{m_1 M-1} \frac{2}{t!\Gamma(m_2)} \left(\frac{\Pi_k}{\bar{\gamma}}\right)^{\frac{m_2+t}{2}} \mathbb{K}_{m_2-t}\left(2\sqrt{\frac{\Pi_k}{\bar{\gamma}}}\right) \sum_{p=0}^{m_1 M-1} \frac{2}{p!\Gamma(m_2 L)} \left(\frac{\Pi_K}{\bar{\gamma}}\right)^{\frac{m_2 L+p}{2}} \mathbb{K}_{m_2 L-p}\left(2\sqrt{\frac{\Pi_K}{\bar{\gamma}}}\right), \quad (21)$$

$$\begin{aligned}\mathbb{P}_{out}^{\text{MES}} = 1 &- \sum_{t=0}^{m_1 M-1} \frac{2}{t!\Gamma(m_2)} \left(\frac{\Pi_1}{\bar{\gamma}}\right)^{\frac{m_2+t}{2}} \mathbb{K}_{t-m_2}\left(2\sqrt{\frac{\Pi_1}{\bar{\gamma}}}\right) \left[1 - \sum_{n=0}^{\infty} \frac{2\chi_{K-1}\psi_E(n, \Omega_{K-1}, N_{K-1})}{\Gamma(m_2 L)} (m_1\Omega_{K-1})^{-n}\right. \\ &\times \left(\frac{\Pi_K N_{K-1}}{\bar{\gamma}}\right)^{\frac{m_2 L - m_1 M N_{K-1} - n}{2}} \left(\frac{\Pi_K}{\bar{\gamma}}\right)^{m_1 M N_{K-1}+n} \mathbb{K}_{m_2 L - m_1 M N_{K-1} - n}\left(2\sqrt{\frac{\Pi_K N_{K-1}}{\bar{\gamma}}}\right)\left.\right] \prod_{k=1}^{K-2} \left[1 - \sum_{n=0}^{\infty} \frac{2\chi_k}{\Gamma(m_2)}\right. \\ &\times \psi_E(n, \Omega_k, N_k)(m_1\Omega_k)^{-n} \left(\frac{\Pi_{k+1} N_k}{\bar{\gamma}}\right)^{\frac{m_2 - m_1 M N_k - n}{2}} \left(\frac{\Pi_{k+1}}{\bar{\gamma}}\right)^{m_1 M N_k + n} \mathbb{K}_{m_2 - m_1 M N_k - n}\left(2\sqrt{\frac{\Pi_{k+1} N_k}{\bar{\gamma}}}\right)\left.\right]. \quad (22)\end{aligned}$$

By applying [27, eq. (0.314)], the CDF of X_b can be obtained in a compact form as

$$F_{X_b}(x) = (m_1\Omega_k x)^{m_1} \exp(-m_1\Omega_k N_k x) \times MN_k \sum_{n=0}^{\infty} \psi_E(n, \Omega_k, N_k) x^n, \quad (30)$$

where $\psi_E(n, \Omega_k, N_k)$ defines for $n > 0$ as

$$\psi_E(n, \Omega_k, N_k) = \frac{\Gamma(m_1 M + 1)}{n} \sum_{\tau=1}^{n} (\tau N_k - n + \tau) \times \frac{(m_1\Omega_k)^{\tau} \psi_E(n-\tau, \Omega_k, N_k)}{\Gamma(m_1 M + 1 + \tau)}, \quad (31)$$

and for $n = 0$ as

$$\psi_E(0, \Omega_k, N_k) = \left[\frac{1}{\Gamma(m_1 M + 1)}\right]^{N_k}. \quad (32)$$

In MES scheme, the selected relay $\mathsf{R}_{k,b}$ having the largest energy will be the forwarder in the next hop; thus, according to the total probability theory [29], the PDF of Y_j in (25) can be calculated as

$$f_{Y_j}(x) = \underbrace{\sum_{i=1}^{N_k} \Pr(\mathsf{R}_{k,b} = \mathsf{R}_{k,i}) f_{|h_{k+1,b,j}|^2}(x)}_{\chi_k}. \quad (33)$$

From (9), we have

$$\begin{aligned}\chi_k &= \sum_{i=1}^{N_k} \Pr\left[\bigcap_{\substack{l=1 \\ l\neq i}}^{N_k} (X_i > X_l)\right] \\ &= \sum_{i=1}^{N_k} \int_0^{+\infty} \underbrace{\prod_{\substack{l=1 \\ l\neq i}}^{N_k} F_{X_l}(x)}_{\Xi} f_{X_i}(x) dx. \quad (34)\end{aligned}$$

From (34), Ξ can be rewritten as

$$\Xi = \left[\frac{\gamma(m_1 M, m_1\Omega_k x)}{\Gamma(m_1 M)}\right]^{N_k - 1}. \quad (35)$$

In the same manner with F_{X_b} in (26), Ξ can be obtained in a compact form as

$$\Xi = (m_1\Omega_k x)^{m_1 M(N_k-1)} \exp(-m_1\Omega_k(N_k-1)x) \times \sum_{u=0}^{\infty} \psi_E(u, \Omega_k, N_k - 1) x^u. \quad (36)$$

Plugging the PDF of X_b, i.e.,

$$f_{X_b}(x) = \frac{(m_1\Omega_k)^{m_1 M} x^{m_1 M - 1}}{\Gamma(m_1 M)} \exp(-m_1\Omega_k x), \quad (37)$$

and Ξ into (34) and after some manipulations, we obtain as

$$\chi_k = \sum_{u=0}^{\infty} \frac{\psi_E(u, \Omega_k, N_k - 1)(m_1\Omega_k)^{-u}}{\Gamma(m_1 M)} \times (N_k)^{1 - m_1 M N_k - u} \Gamma(m_1 M N_k + u). \quad (38)$$

Then, substituting $f_{|h_{k+1,b,j}|^2}(x)$ and χ_k into (33), we obtain as

$$f_{Y_j}(x) = \chi_k \frac{(m_2\lambda_{k+1})^{m_2} x^{m_2 - 1}}{\Gamma(m_2)} \exp(-m_2\lambda_{k+1} x). \quad (39)$$

Plugging (39) and (30) into (25) and then using of [27, eq. (3.471.9)], we obtain the CDF of $\gamma_{k+1,b,j}^{\text{MES}}$ as

$$\begin{aligned}F_{\gamma_{k+1,b,j}^{\text{MES}}}(\gamma_{\text{th}}) = \sum_{n=0}^{\infty} &\frac{2\chi_k \psi_E(n, \Omega_k, N_k)}{\Gamma(m_2)} \left(\frac{\Pi_{k+1}}{\bar{\gamma}}\right)^{m_1 M N_k + n} \\ &\times (m_1\Omega_k)^{-n} \left(\frac{\Pi_{k+1} N_k}{\bar{\gamma}}\right)^{\frac{m_2 - m_1 M N_k - n}{2}} \\ &\times \mathbb{K}_{m_2 - m_1 M N_k - n}\left(2\sqrt{\frac{\Pi_{k+1} N_k}{\bar{\gamma}}}\right). \quad (40)\end{aligned}$$

In the last hop, let $X_{\mathsf{D}} = \max_{i=1,\ldots,N_{K-1}} \sum_{m=1}^{M} |g_{K-1,m,i}|^2$ and $Z = \sum_{l=1}^{L} |h_{\mathsf{D},l}|^2$, the CDF of $\gamma_{\mathsf{D}}^{\text{MES}}$ can be calculated as

$$\begin{aligned}F_{\gamma_{\mathsf{D}}^{\text{MES}}}(\gamma_{\text{th}}) &= \Pr[\kappa\bar{\gamma} X_{\mathsf{D}} Z < \gamma_{\text{th}}] \\ &= \int_0^{+\infty} F_{X_{\mathsf{D}}}\left(\frac{\gamma_{\text{th}}}{\kappa\bar{\gamma} x}\right) f_Z(x) dx. \quad (41)\end{aligned}$$

$$\mathbb{P}_{out}^{\mathrm{MDS}} = 1 - \sum_{t=0}^{m_1M-1} \frac{2\Theta_{K-1}}{t!\Gamma(m_2L)} \left(\frac{\Pi_K}{\bar{\gamma}}\right)^{\frac{m_2L+t}{2}} \mathbb{K}_{m_2L-t}\left(2\sqrt{\frac{\Pi_K}{\bar{\gamma}}}\right) \prod_{k=1}^{K-1} \left[1 - \sum_{n=0}^{\infty} \frac{2\Theta_{k-1}}{\Gamma(m_1M)} \left(\frac{\Pi_k}{\bar{\gamma}}\right)^{m_2N_k+n} \times (m_2\lambda_k)^{-n} \psi_D(n, \lambda_k, N_k) \left(\frac{\Pi_k N_k}{\bar{\gamma}}\right)^{\frac{m_1M-m_2N_k-n}{2}} \mathbb{K}_{m_1M-m_2N_k-n}\left(2\sqrt{\frac{\Pi_k N_k}{\bar{\gamma}}}\right)\right]. \quad (45)$$

Similar to (30), we have the CDF of X_{D} given as

$$F_{X_{\mathsf{D}}}(x) = (m_1\Omega_{K-1}x)^{m_1MN_{K-1}} \exp(-m_1\Omega_{K-1}N_{K-1}x) \times \sum_{n=0}^{\infty} \psi_E(n, \Omega_{K-1}, N_{K-1})x^n. \quad (42)$$

Since D employs MRC technique to combine the received signals from the best energy relay in cluster $K-1$. Therefore, the PDF of Z is given as

$$f_Z(x) = \chi_{K-1} \frac{(m_2\lambda_K)^{m_2L} x^{m_2L-1}}{\Gamma(m_2L)} \exp(-m_2\lambda_K x). \quad (43)$$

Substituting (42) and (43) into (41) and then using [27, eq. (3.471.9)], we obtain as

$$F_{\gamma_{\mathsf{D}}^{\mathrm{MES}}}(\gamma_{\mathrm{th}}) = \sum_{n=0}^{\infty} \frac{2\chi_{K-1}\psi_E(n, \Omega_{K-1}, N_{K-1})}{\Gamma(m_2L)} \times (m_1\Omega_{K-1})^{-n} \left(\frac{\Pi_K}{\bar{\gamma}}\right)^{m_1MN_{K-1}+n} \times \left(\frac{\Pi_K N_{K-1}}{\bar{\gamma}}\right)^{\frac{m_2L-m_1MN_{K-1}-n}{2}} \times \mathbb{K}_{-m_2L+m_1MN_{K-1}+n}\left(2\sqrt{\frac{\Pi_K N_{K-1}}{\bar{\gamma}}}\right). \quad (44)$$

Plugging (24), (40) and (44) into (23), we obtain the desired result as (22), which also finish the proof here. ■

C. MDS SCHEME

Theorem 3: The exact closed-form expression of the outage probability for MDS protocol over Nakagami-m fading channels is given as (45), shown at the top of this page.

Proof: The outage probability of the MDS protocol can be rewritten as

$$\mathbb{P}_{out}^{\mathrm{MDS}} = 1 - \left[1 - F_{\gamma_{\mathsf{D}}^{\mathrm{MDS}}}(\gamma_{\mathrm{th}})\right] \prod_{k=1}^{K-1} \left[1 - F_{\gamma_{k,b,j}^{\mathrm{MDS}}}(\gamma_{\mathrm{th}})\right], \quad (46)$$

where $F_{\gamma_{k,b,j}^{\mathrm{MDS}}}(.)$ and $F_{\gamma_{\mathsf{D}}^{\mathrm{MDS}}}(.)$ are the CDF of $\gamma_{k,b,j}^{\mathrm{MDS}}$ and $\gamma_{\mathsf{D}}^{\mathrm{MDS}}$, respectively.

For the sake of simplicity, let $X = \sum_{m=1}^{M} |g_{k-1,m,b}|^2$ and $Y = \max_{j=1,\ldots,N_k} |h_{k,b,j}|^2$. $F_{\gamma_{k,b,j}^{\mathrm{MDS}}}(\gamma_{\mathrm{th}})$ can be calculated as

$$F_{\gamma_{k,b,j}^{\mathrm{MDS}}}(\gamma_{\mathrm{th}}) = \Pr[\kappa\bar{\gamma}XY < \gamma_{\mathrm{th}}] = \int_0^{+\infty} F_Y\left(\frac{\gamma_{\mathrm{th}}}{\kappa\bar{\gamma}x}\right) f_X(x)dx. \quad (47)$$

In MDS scheme, the best relay $\mathsf{R}_{k-1,b}$ is selected by the strategy (12) to forward the re-encoded signal to the relay in cluster k. Using the total probability theorem [29], the CDF of Y can be calculated as

$$F_Y(x) = \underbrace{\Pr\left[\max_{j=1,\ldots,N_k} |h_{k,b,j}|^2 < x\right]}_{\Phi} \times \underbrace{\sum_{i=1}^{N_{k-1}} \Pr(\mathsf{R}_{k-1,b} = \mathsf{R}_{k-1,i})}_{\Theta_{k-1}}. \quad (48)$$

Invoking the similar approach in the proof of Theorem 2, Φ can be easily obtained in a compact form as

$$\Phi = (m_2\lambda_k x)^{m_2N_k} \exp(-m_2N_k\lambda_k x) \times \sum_{n=0}^{\infty} \psi_D(n, \lambda_k, N_k)x^n, \quad (49)$$

where $\psi_D(n, \lambda_k, N_k)$ is defined for $n > 0$ as

$$\psi_D(n, \lambda_k, N_k) = \frac{\Gamma(m_2+1)}{n} \sum_{\tau=1}^{n} (\tau N_k - n + \tau) \times \frac{(m_2\lambda_k)^{\tau}}{\Gamma(m_2+1+\tau)} \psi_D(n-\tau, \lambda_k, N_k), \quad (50)$$

and for $n = 0$ as

$$\psi_D(0, \lambda_k, N_k) = \left[\frac{1}{\Gamma(m_2+1)}\right]^{N_k}. \quad (51)$$

Similar to the derived steps of χ_k as in (33), Θ_{k-1} can be obtained as

$$\Theta_{k-1} = \sum_{u=0}^{\infty} \frac{\psi_D(u, \lambda_{k-1}, N_{k-1}-1)(m_2\lambda_{k-1})^{-u}}{\Gamma(m_2)} \times (N_{k-1})^{1-u-m_2N_{k-1}} \Gamma(m_2N_{k-1}+u). \quad (52)$$

Substituting (49) and (52) into (48), we can easily obtain $F_Y(x)$ as

$$F_Y(x) = \Theta_{k-1}(m_2\lambda_k x)^{m_2N_k} \exp(-m_2N_k\lambda_k x) \times \sum_{n=0}^{\infty} \psi_D(n, \lambda_k, N_k)x^n. \quad (53)$$

Plugging (53) and $f_X(x)$ into (47) and then using again of [27, eq. (3.471.9)], $F_{\gamma_{k,b,j}^{\mathrm{MDS}}}$ can be obtained as

$$F_{\gamma_{k,b,j}^{\mathrm{MDS}}}(\gamma_{\mathrm{th}}) = \sum_{n=0}^{\infty} \frac{2\psi_D(n, \lambda_k, N_k)\Theta_{k-1}}{\Gamma(m_1M)} \left(\frac{\Pi_k}{\bar{\gamma}}\right)^{m_2N_k+n}$$

$$\times (m_2\lambda_k)^{-n}\left(\frac{\Pi_k N_k}{\bar{\gamma}}\right)^{\frac{m_1M-m_2N_k-n}{2}} \times \mathbb{K}_{m_1M-m_2N_k-n}\left(2\sqrt{\frac{\Pi_k N_k}{\bar{\gamma}}}\right). \quad (54)$$

In the last hop, let $X_{\mathsf{D}} = \sum_{m=1}^{M} |g_{K-1,m,b}|^2$ and $Z = \sum_{l=1}^{L} |h_{\mathsf{D},l}|^2$, the CDF of $\gamma_{\mathsf{D}}^{\mathrm{MDS}}$ can be calculated as

$$F_{\gamma_{\mathsf{D}}^{\mathrm{MDS}}}(\gamma_{\mathrm{th}}) = \Pr\left[\kappa\bar{\gamma}X_{\mathsf{D}}Z < \gamma_{\mathrm{th}}\right] = \int_0^{+\infty} F_{X_{\mathsf{D}}}\left(\frac{\gamma_{\mathrm{th}}}{\kappa\bar{\gamma}x}\right) f_Z(x)dx. \quad (55)$$

Plugging the CDF of X_{D}, i.e.,

$$F_{X_{\mathsf{D}}}(x) = 1 - \exp(-m_1\Omega_{K-1}x) \times \sum_{t=0}^{m_1M-1} \frac{(m_1\Omega_{K-1}x)^t}{t!}, \quad (56)$$

and the PDF of Z, i.e.,

$$f_Z(x) = \Theta_{K-1}\frac{(m_2\lambda_K)^{m_2L}x^{m_2L-1}}{\Gamma(m_2L)}\exp(-m_2\lambda_K x), \quad (57)$$

into (55) and applying of [27, eq.(3.471.9)], we obtain as

$$F_{\gamma_{\mathsf{D}}^{\mathrm{MDS}}}(\gamma_{\mathrm{th}}) = 1 - \sum_{t=0}^{m_1M-1}\frac{2}{t!}\left(\frac{\Pi_K}{\bar{\gamma}}\right)^{\frac{m_2L+t}{2}} \times \frac{\Theta_{K-1}}{\Gamma(m_2L)}\mathbb{K}_{m_2L-t}\left(2\sqrt{\frac{\Pi_K}{\bar{\gamma}}}\right). \quad (58)$$

Plugging (54) and (58) into (46), we obtain the desired result as (45), the proof is concluded. ■

D. MEDS SCHEME

In this scheme, the system outage probability is considered in two cases as follows:

Case 1: The number of clusters is even

Theorem 4: The exact closed-form expression of the outage probability for MEDS scheme over Nakagami-*m* fading channels is given as (59), shown at the top of the next page.

Proof: The outage probability of the MEDS protocol for Case 1 can be rewritten as

$$\mathbb{P}_{out}^{\mathrm{MEDS}} = 1 - [1 - F_{\gamma_{1,j,b}^{\mathrm{MEDS}}}(\gamma_{\mathrm{th}})][1 - F_{\gamma_{\mathsf{D}}^{\mathrm{MEDS}}}(\gamma_{\mathrm{th}})] \times \prod_{k=2}^{(K-1)/2}[1 - F_{\gamma_{k,j,b}^{\mathrm{MEDS}}}(\gamma_{\mathrm{th}})]. \quad (60)$$

Firstly, the CDF of $\gamma_{1,j,b}^{\mathrm{MEDS}}$ can be calculated as

$$F_{\gamma_{1,j,b}^{\mathrm{MEDS}}}(\gamma_{\mathrm{th}}) = \underbrace{\sum_{i=1}^{N_2}\Pr\left[\mathsf{R}_{2,b} = \mathsf{R}_{2,i}\right]}_{\chi_2} \times \prod_{j=1}^{N_1}\underbrace{\Pr\left[\min\left\{X_1^M, Y_1^M\right\} < \gamma_{\mathrm{th}}\right]}_{\Delta_1}, \quad (61)$$

where $X_1 = \sum_{m=1}^{M}\kappa\bar{\gamma}|g_{0,m,1}|^2|h_{1,i,j}|^2$ and $Y_1 = \sum_{m=1}^{M}\kappa\bar{\gamma}|g_{1,m,j}|^2|h_{2,j,b}|^2$.

Invoking (38) with $k = 2$, we obtain χ_2 as

$$\chi_2 = \sum_{u=0}^{\infty}\frac{\psi_E(u, \Omega_2, N_2 - 1)(m_1\Omega_2)^{-u}}{\Gamma(m_1M)} \times (N_2)^{1-m_1MN_2-u}\Gamma(m_1MN_2 + u). \quad (62)$$

Since X_1 and Y_1 are independent, Δ_1 in (61) can be rewritten as follows:

$$\Delta_1 = 1 - [1 - F_{X_1}(\gamma_{\mathrm{th}})][1 - F_{Y_1}(\gamma_{\mathrm{th}})]. \quad (63)$$

Recalling the Theorem 1, $F_{X_1}(\gamma_{\mathrm{th}})$ can be obtained as

$$F_{X_1}(\gamma_{\mathrm{th}}) = 1 - \sum_{t=0}^{m_1M-1}\frac{2}{t!\Gamma(m_2)}\left(\frac{\Pi_1}{\bar{\gamma}}\right)^{\frac{m_2+t}{2}} \times \mathbb{K}_{m_2-t}\left(2\sqrt{\frac{\Pi_1}{\bar{\gamma}}}\right), \quad (64)$$

and CDF of Y_1 is obtained as

$$F_{Y_1}(\gamma_{\mathrm{th}}) = 1 - \sum_{p=0}^{m_1M-1}\frac{2}{p!\Gamma(m_2)}\left(\frac{\Pi_2}{\bar{\gamma}}\right)^{\frac{m_2+p}{2}} \times \mathbb{K}_{m_2-p}\left(2\sqrt{\frac{\Pi_2}{\bar{\gamma}}}\right). \quad (65)$$

From (62), (64) and (65), the CDF of $\gamma_{1,j,b}^{\mathrm{MEDS}}$ can be obtained as

$$F_{\gamma_{1,j,b}^{\mathrm{MEDS}}}(\gamma_{\mathrm{th}}) = \chi_2\left[1 - \sum_{t=0}^{m_1M-1}\frac{2}{t!\Gamma(m_2)}\left(\frac{\Pi_1}{\bar{\gamma}}\right)^{\frac{m_2+t}{2}} \times \mathbb{K}_{m_2-t}\left(2\sqrt{\frac{\Pi_1}{\bar{\gamma}}}\right)\sum_{p=0}^{m_1M-1}\frac{2}{p!\Gamma(m_2)} \times \left(\frac{\Pi_2}{\bar{\gamma}}\right)^{\frac{m_2+p}{2}}\mathbb{K}_{m_2-p}\left(2\sqrt{\frac{\Pi_2}{\bar{\gamma}}}\right)\right]^{N_1}. \quad (66)$$

Next, the CDF of γ_k^M can be calculated as

$$F_{\gamma_k^M}(\gamma_{\mathrm{th}}) = \underbrace{\sum_{i=1}^{N_{2k}}\Pr\left[\mathsf{R}_{2k,b} = \mathsf{R}_{2k,i}\right]}_{\chi_{2k}} \times \prod_{j=1}^{N_{2k-1}}\underbrace{\Pr\left[\min\left\{X_k^M, Y_k^M\right\} < \gamma_{\mathrm{th}}\right]}_{\Delta_k}, \quad (67)$$

where $X_k = \max_{i=1,\ldots,N_{2k-2}}\sum_{m=1}^{M}\kappa\bar{\gamma}|g_{2k-2,m,i}|^2|h_{2k-1,i,j}|^2$ and $Y_k = \sum_{m=1}^{M}\kappa\bar{\gamma}|g_{2k-1,m,j}|^2|h_{2k,j,b}|^2$.

$$\mathbb{P}_{out,even}^{\text{MEDS}} = 1 - \left(1 - \chi_2 \left[1 - \sum_{t=0}^{m_1M-1} \frac{2}{t!\Gamma(m_2)} \left(\frac{\Pi_1}{\bar{\gamma}}\right)^{\frac{m_2+t}{2}} \mathbb{K}_{m_2-t}\left(2\sqrt{\frac{\Pi_1}{\bar{\gamma}}}\right) \sum_{p=0}^{m_1M-1} \frac{2}{p!\Gamma(m_2)} \right.\right.$$
$$\times \left.\left(\frac{\Pi_2}{\bar{\gamma}}\right)^{\frac{m_2+p}{2}} \mathbb{K}_{m_2-p}\left(2\sqrt{\frac{\Pi_2}{\bar{\gamma}}}\right)\right]^{N_1}\Bigg) \left(1 - \sum_{n=0}^{\infty} \frac{2\psi_E\left(n, \Omega_{K-1}, N_{K-1}\right)\left(m_1\Omega_{K-1}\right)^{-n}\chi_{K-1}}{\Gamma(m_2L)} \right.$$
$$\times \left(\frac{\Pi_K}{\bar{\gamma}}\right)^{m_1MN_{K-1}+n} \left(\frac{\Pi_K N_{K-1}}{\bar{\gamma}}\right)^{\frac{m_2L-m_1MN_{K-1}-n}{2}} \mathbb{K}_{m_2L-m_1MN_{K-1}-n}\left(2\sqrt{\frac{\Pi_K N_{K-1}}{\bar{\gamma}}}\right)\Bigg)$$
$$\times \prod_{k=2}^{(K-1)/2} \left(1 - \chi_{2k}\left[1 - \left(1 - \sum_{n=0}^{\infty} \frac{2\psi_E\left(n, \Omega_{2k}, N_{2k}\right)\chi_{2k-2}}{\Gamma(m_2)} \left(\frac{\Pi_{2k-1}}{\bar{\gamma}}\right)^{m_1MN_{2k-2}+n} \right.\right.\right.$$
$$\times \left.\left.\left(m_1\Omega_{2k-2}\right)^{-n}\left(\frac{\Pi_{2k-1}N_{2k-2}}{\bar{\gamma}}\right)^{\frac{m_2-m_1MN_{2k-2}-n}{2}} \mathbb{K}_{m_2-m_1MN_{2k-2}-n}\left(2\sqrt{\frac{\Pi_{2k-1}N_{2k-2}}{\bar{\gamma}}}\right)\right)$$
$$\times \left.\left.\sum_{t=0}^{m_1M-1} \frac{2}{t!\Gamma(m_2)} \left(\frac{\Pi_{2k}}{\bar{\gamma}}\right)^{\frac{m_2+t}{2}} \mathbb{K}_{m_2-t}\left(2\sqrt{\frac{\Pi_{2k}}{\bar{\gamma}}}\right)\right]^{N_{2k-1}}\right). \tag{59}$$

From (67), χ_{2k} can be easily obtained as

$$\chi_{2k} = \sum_{u=0}^{\infty} \frac{\psi_E(u, \Omega_{2k}, N_{2k}-1)(m_1\Omega_{2k})^{-u}}{\Gamma(m_1M)} \times (N_{2k})^{1-m_1MN_{2k}-u}\Gamma(m_1MN_{2k}+u), \tag{68}$$

and Δ_k can be rewritten as

$$\Delta_k = 1 - \left[1 - F_{X_k^M}(\gamma_{\text{th}})\right]\left[1 - F_{Y_k^M}(\gamma_{\text{th}})\right]. \tag{69}$$

Similar to the proof of Theorem 2, $F_{X_k}(\gamma_{\text{th}})$ can be obtained as

$$F_{X_k}(\gamma_{\text{th}}) = \sum_{n=0}^{\infty} \frac{2\psi_E(n, \Omega_{2k}, N_{2k})}{\Gamma(m_2)} \left(\frac{\Pi_{2k-1}}{\bar{\gamma}}\right)^{m_1MN_{2k-2}+n} \times (m_1\Omega_{2k-2})^{-n}\left(\frac{\Pi_{2k-1}N_{2k-2}}{\bar{\gamma}}\right)^{\frac{m_2-m_1MN_{2k-2}-n}{2}} \times \chi_{2k-2}\mathbb{K}_{m_2-m_1MN_{2k-2}-n}\left(2\sqrt{\frac{\Pi_{2k-1}N_{2k-2}}{\bar{\gamma}}}\right), \tag{70}$$

and $F_{Y_k}(\gamma_{\text{th}})$ is obtained as

$$F_{Y_k}(\gamma_{\text{th}}) = 1 - \sum_{t=0}^{m_1M-1} \frac{2}{t!\Gamma(m_2)} \left(\frac{\Pi_{2k}}{\bar{\gamma}}\right)^{\frac{m_2+t}{2}} \times \mathbb{K}_{m_2-t}\left(2\sqrt{\frac{\Pi_{2k}}{\bar{\gamma}}}\right). \tag{71}$$

In the last hop, similarly to the MES scheme, the CDF of γ_K^M can be easily obtained as

$$F_{\gamma_{\text{D}}^{\text{MEDS}}}(\gamma_{\text{th}}) = \sum_{n=0}^{\infty} \frac{2\psi_E(n, \Omega_{K-1}, N_{K-1})(m_1\Omega_{K-1})^{-n}}{\Gamma(m_2L)} \times \chi_{K-1}\left(\frac{\Pi_K}{\bar{\gamma}}\right)^{m_1MN_{K-1}+n} \times \left(\frac{\Pi_K N_{K-1}}{\bar{\gamma}}\right)^{\frac{m_2L-m_1MN_{K-1}-n}{2}} \times \mathbb{K}_{n-m_2L+m_1MN_{K-1}}\left(2\sqrt{\frac{\Pi_K N_{K-1}}{\bar{\gamma}}}\right). \tag{72}$$

Having $F_{\gamma_{1,j,b}^{\text{MEDS}}}(.)$, $F_{\gamma_{k,j,b}^{\text{MEDS}}}(.)$ and $F_{\gamma_{\text{D}}^{\text{MEDS}}}(.)$ at hands, plugging every things into (60), we obtain the desired result as (59), the proof is concluded. ■

Case 2: The number of clusters is odd

Theorem 5: The exact closed-form expression of the outage probability for MEDS scheme when over Nakagami-*m* fading channels is given as (73), shown at the top of the next page.

Proof: The outage probability of the MEDS protocol for Case 2 can be rewritten as

$$\mathbb{P}_{out}^{\text{MEDS}} = 1 - [1 - F_{\gamma_{1,j,b}^{\text{MEDS}}}(\gamma_{\text{th}})][1 - F_{\gamma_{2,j,b}^{\text{MEDS}}}(\gamma_{\text{th}})] \times [1 - F_{\gamma_{\text{D}}^{\text{MEDS}}}(\gamma_{\text{th}})] \prod_{k=1}^{(K-4)/2} [1 - F_{\gamma_{k,j,b}^{\text{MEDS}}}(\gamma_{\text{th}})]. \tag{74}$$

Invoking the Theorem 3, the CDF of $\gamma_{1,j,b}^{\text{MEDS}}$ can be obtained as

$$F_{\gamma_{1,j,b}^{\text{MEDS}}}(\gamma_{\text{th}}) = \sum_{n=0}^{\infty} \frac{2\psi_D(n, \lambda_1, N_1)}{\Gamma(m_1M)} \left(\frac{\Pi_1}{\bar{\gamma}}\right)^{m_2N_1+n} \times (m_2\lambda_1)^{-n}\left(\frac{\Pi_1 N_1}{\bar{\gamma}}\right)^{\frac{m_1M-m_2N_1-n}{2}} \times \mathbb{K}_{m_1M-m_2N_1-n}\left(2\sqrt{\frac{\Pi_1 N_1}{\bar{\gamma}}}\right). \tag{75}$$

$$\mathbb{P}_{out,odd}^{\text{MEDS}} = 1 - \Bigg[1 - \sum_{n=0}^{\infty} \frac{2\psi_D(n,\lambda_1,N_1)}{\Gamma(m_1M)} \left(\frac{\Pi_1}{\bar{\gamma}}\right)^{m_2N_1+n} (m_2\lambda_1)^{-n} \left(\frac{\Pi_1 N_1}{\bar{\gamma}}\right)^{\frac{m_1M-m_2N_1-n}{2}} \times \mathbb{K}_{m_1M-m_2N_1-n}\left(2\sqrt{\frac{\Pi_1 N_1}{\bar{\gamma}}}\right)\Bigg] \Bigg[1 - \Theta_1\chi_3 \Bigg(1 - \sum_{t=0}^{m_1M-1} \frac{2}{t!\Gamma(m_2)} \left(\frac{\Pi_2}{\bar{\gamma}}\right)^{\frac{m_2+t}{2}} \times \mathbb{K}_{m_2-t}\left(2\sqrt{\frac{\Pi_2}{\bar{\gamma}}}\right) \sum_{p=0}^{m_1M-1} \frac{2}{p!\Gamma(m_2)} \left(\frac{\Pi_3}{\bar{\gamma}}\right)^{\frac{m_2+p}{2}} \mathbb{K}_{m_2-p}\left(2\sqrt{\frac{\Pi_3}{\bar{\gamma}}}\right)\Bigg)^{N_2}\Bigg] \times \Bigg[1 - \sum_{n=0}^{\infty} \frac{2\psi_E(n,\Omega_{K-1},N_{K-1})}{\Gamma(m_2L)} (m_1\Omega_{K-1})^{-n} \left(\frac{\Pi_K N_{K-1}}{\bar{\gamma}}\right)^{\frac{m_2L-m_1MN_{K-1}-n}{2}} \times \chi_{K-1}\left(\frac{\Pi_K}{\bar{\gamma}}\right)^{\frac{m_1MN_{K-1}+n}{2}} \mathbb{K}_{n-m_2L+m_1MN_{K-1}}\left(2\sqrt{\frac{\Pi_K N_{K-1}}{\bar{\gamma}}}\right)\Bigg] \times \prod_{k=1}^{(K-4)/2} \Bigg[1 - \chi_{2k}\Bigg(1 - \sum_{t=0}^{m_1M-1} \frac{2}{t!\Gamma(m_2)} \left(\frac{\Pi_{2k}}{\bar{\gamma}}\right)^{\frac{m_2+t}{2}} \mathbb{K}_{m_2-t}\left(2\sqrt{\frac{\Pi_{2k}}{\bar{\gamma}}}\right) \times \Bigg[1 - \sum_{n=0}^{\infty} \frac{2\psi_E(n,\Omega_{2k},N_{2k})\,\chi_{2k-2}}{\Gamma(m_2)} \left(\frac{\Pi_{2k-1}}{\bar{\gamma}}\right)^{m_1MN_{2k-2}+n} (m_1\Omega_{2k-2})^{-n} \times \left(\frac{\Pi_{2k-1}N_{2k-2}}{\bar{\gamma}}\right)^{\frac{m_2-m_1MN_{2k-2}-n}{2}} \mathbb{K}_{m_2-m_1MN_{2k-2}-n}\left(2\sqrt{\frac{\Pi_{2k-1}N_{2k-2}}{\bar{\gamma}}}\right)\Bigg]\Bigg)^{N_{2k-1}}\Bigg]. \quad (73)$$

Next, the CDF of $\gamma_{2,j,b}^{\text{MEDS}}$ can be calculated as

$$F_{\gamma_{2,j,b}^{\text{MEDS}}}(\gamma_{\text{th}}) = \underbrace{\sum_{i=1}^{N_1} \Pr\left[\mathsf{R}_{1,b} = \mathsf{R}_{1,i}\right]}_{\Theta_1} \underbrace{\sum_{l=1}^{N_3} \Pr\left[\mathsf{R}_{3,b} = \mathsf{R}_{3,l}\right]}_{\chi_3} \times \prod_{j=1}^{N_2} \underbrace{\Pr\left[\min\left\{X_2^M, Y_2^M\right\} < \gamma_{\text{th}}\right]}_{\Delta_2}, \quad (76)$$

where $X_2 = \sum_{m=1}^{M} \kappa\bar{\gamma}|g_{1,m,b}|^2|h_{2,b,j}|^2$ and $Y_2 = \sum_{m=1}^{M} \kappa\bar{\gamma}|g_{2,m,j}|^2|h_{3,j,b}|^2$.

Since X_2 and Y_2 are independent, Δ_2 can be rewritten as

$$\Delta_2 = 1 - \left[1 - F_{X_2}(\gamma_{\text{th}})\right]\left[1 - F_{Y_2}(\gamma_{\text{th}})\right]. \quad (77)$$

Invoking the Theorem 1, $F_{X_2}(\gamma_{\text{th}})$ can be obtained as

$$F_{X_2}(\gamma_{\text{th}}) = 1 - \sum_{t=0}^{m_1M-1} \frac{2}{t!\Gamma(m_2)} \left(\frac{\Pi_2}{\bar{\gamma}}\right)^{\frac{m_2+t}{2}} \times \mathbb{K}_{m_2-t}\left(2\sqrt{\frac{\Pi_2}{\bar{\gamma}}}\right), \quad (78)$$

and the CDF of Y_2 is obtained as

$$F_{Y_2}(\gamma_{\text{th}}) = 1 - \sum_{p=0}^{m_1M-1} \frac{2}{p!\Gamma(m_2)} \left(\frac{\Pi_3}{\bar{\gamma}}\right)^{\frac{m_2+p}{2}} \times \mathbb{K}_{m_2-p}\left(2\sqrt{\frac{\Pi_3}{\bar{\gamma}}}\right). \quad (79)$$

Next, $F_{\gamma_{k,j,b}^{\text{MEDS}}}(.)$ and $F_{\gamma_{\text{D}}^{\text{MEDS}}}(.)$ can be obtained similarly to (67) and (72) as in Case 1, respectively.

Having $F_{\gamma_{1,j,b}^{\text{MEDS}}}(.)$,$F_{\gamma_{2,j,b}^{\text{MEDS}}}(.)$, $F_{\gamma_{k,j,b}^{\text{MEDS}}}(.)$and $F_{\gamma_{\text{D}}^{\text{MEDS}}}(.)$ at hands, plugging every things into (74), we obtain the desired result as (73), the proof is concluded. ■

TABLE 2. Simulation parameters.

Parameters	Value
The distance between S and D, d_{SD}	10 meters
The reference distance, d_0	1 meter
The position of S	$(0, 0)$
The position of $\mathsf{R}_{k,i}$	$(k/K, 0)$
The position of D	$(10, 0)$
The position of PB_m	$(7.5, 5.5)$
Target data rate $\mathcal{R}_{\text{th}}$	1 bits/s/Hz
The shape parameters, m_1 and m_2.	2
Pathloss exponent, β	2.4
Energy conversion efficiency, η	0.7
Pathloss at reference distance, ($\mathcal{L}$ at d_0)	-30 dB

IV. NUMERICAL RESULTS AND DISCUSSIONS

In this section, Monte-Carlo simulations results are provided to verify the analytical expressions. The simulation parameters are presented in Table 2. In this paper, the first 20 terms truncated for the multinomial coefficients, $\psi_E(n, \Omega_k, N_k)$ and $\psi_D(n, \lambda_k, N_k)$, will be used to obtain the accurate outage probability of MES, MDS and MEDS schemes.

We first study the effects of the number of PBs on the system outage performance. As shown in Fig. 6 that

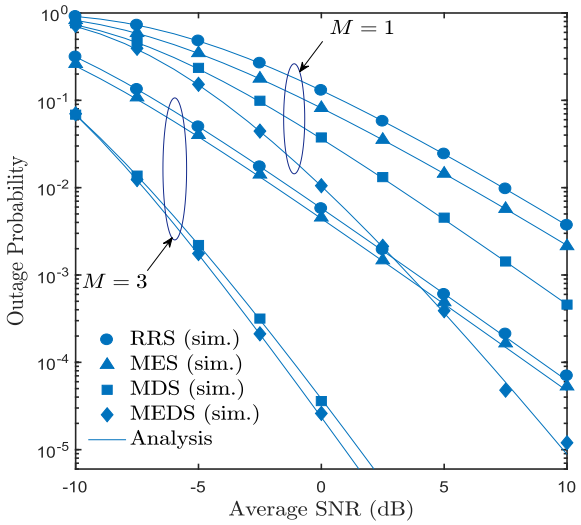

FIGURE 6. Effects of the number of PBs on the system OP with $K = 6$, $\alpha = 0.2$, $N_k = 2$ and $L = 3$.

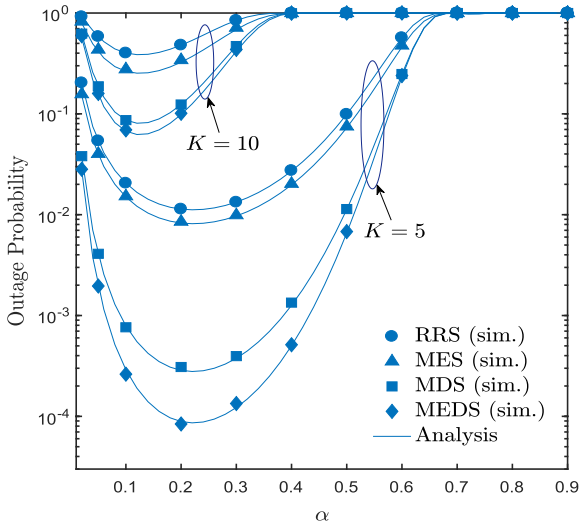

FIGURE 7. Effects of α on the system OP with $\bar{\gamma} = 1$ dB, $N_k = 2$ and $L = 3$.

increasing the number of PBs or growing average SNRs leads to the considerable improvement performance of all schemes, the relay nodes have more opportunity to harvest energy from RF radiation. Moreover, Fig. 6 shows that with the same channel configurations, the MEDS scheme provides the best performance among those of MDS, MES and RRS schemes, as expected. For example, we consider the outage probability at the value of 10^{-1} with $M = 1$, the MEDS scheme provides 1.5 dB, 2.5 dB and 4.0 dB gain as compared with MDS, MES and RRS schemes, respectively. In addition, when increasing the number of PBs, the performance gap between MEDS and MES schemes significantly increases while the gap between MEDS and MDS schemes slightly reduces. This indicates that the number of PBs plays an important role in the relay selection scheme based on data channel gain, i.e., MEDS and MDS schemes. It can be further noticed that MEDS outperforms MDS schemes but the MEDS scheme requires more CSI estimations than that of MDS scheme. This is due to the fact that the MDS scheme selects the best relay based on the CSI of the channel from transmitter to relay in the received cluster while the MEDS generally considers the CSI of both channels from transmitter to relay in the received cluster and from this cluster to relay in the next cluster. Therefore, MEDS scheme increases the system overhead but it provides the better reception reliability than MDS scheme. Fig. 6 also presents that the theoretical results agrees excellently with the simulation ones, confirming the correctness of our derivation approach.

Fig. 7 plots the outage probability of RRS, MES, MDS and MEDS schemes as a function of time switching ratio α with different value of hops. It can be observed, the system outage probability is a convex function of α and the optimal time switching ratio, α_{opt}, considerably depends on the number of hops. Moreover, α_{opt} is unaffected by the relay selection strategies, i.e., RRS, MES, MDS and MEDS schemes, and it takes the same value for each scheme in multi-hop fashion.

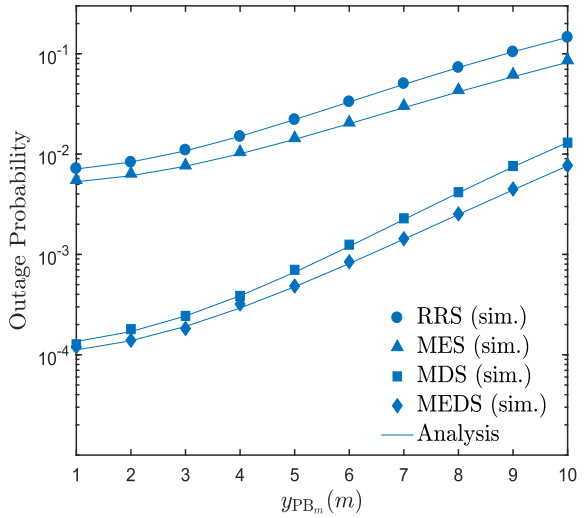

FIGURE 8. Effects of the PBs position on the system OP with $K = 6$, $x_{\text{PB}_m} = 7.5$ m, $\alpha = 0.4$, $L = 2$ and $N_k = 2$.

Furthermore, α_{opt} tends to decrease with increasing number of hops, K, since the system requires more time for relaying data resulting in the decrease of energy harvesting time. When the value of α is greater than 0.7, the system outage probability of all schemes seems to be saturated. Therefore, we can conclude that (i) choosing α is more important than choosing K and (ii) α_k is shown as a complicated function of the related system parameters including number of relays in each cluster, number of hops, number of antennas at D and average $\bar{\gamma}$. In addition, the system OP of MEDS scheme provides the best performance among remaining schemes, which shows the advantages of relay selection strategy employing in MEDS scheme.

Fig. 8 reveals that the PBs position plays an important role on the system performance. To provide insight information of the effects of PBs position on the system OP, we vary the

y-coordinate of the PBs from 1 m to 10 m, when $x_{\mathrm{PB}_m} = 7.5$ m and $\bar{\gamma} = 10$ dB. As can be observed, the distance between PBs and multi-hop network rises, the system OP increases. This results can be explained by considering the fact that the energy harvesting at each relay is also a function of pathloss. Moreover, MEDS scheme is more robust than remaining schemes since the energy harvesting relay selection cooperates with the opportunistic relay selection to overcome the pathloss attenuation. In addition, the system outage performances of RRS, MES, MDS and MEDS can be improved by locating the PBs closely to the network, i.e., along multi-hop networks.

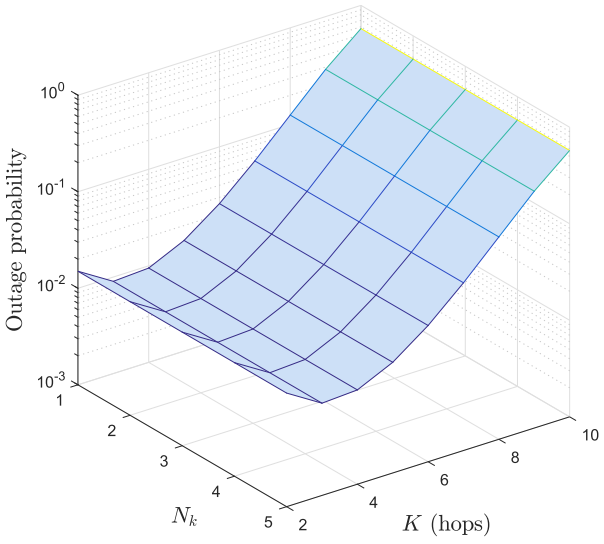

FIGURE 9. Effects of the number of hops and number of relays on the OP of RRS scheme with $\bar{\gamma} = -2$ dB, $M = 3$ and $L = 3$.

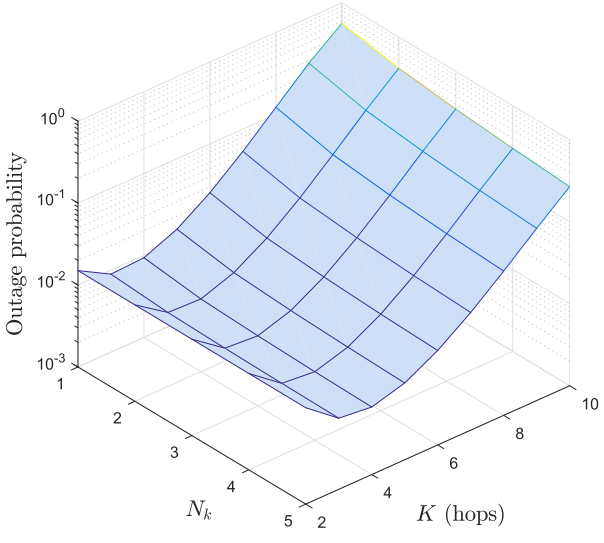

FIGURE 10. Effects of the number of hops and number of relays on the OP of MES scheme with $\bar{\gamma} = -2$ dB, $M = 3$ and $L = 3$.

From Fig. 9 to Fig. 12, we study the effects of the number of relays and the number of hops on outage probability of RRS, MES, MDS and MEDS schemes, respectively. As we can see in Fig. 10 to Fig. 12, the improvement of the system outage performance will be proportional to the number of relays in MES, MDS and MEDS schemes since more relays take part in the relaying operation and hence the outage probability decreases. In Fig. 9, increasing the number of relay does not impact on the system OP since the RRS scheme based on the single-relay selection. In Fig. 10 and Fig. 11, the system OP of MDS scheme significantly decreases while the system OP of MES scheme slightly reduces. We can conclude that with the multi-hop cluster-based system, the data channel gain based relay selection dominates the energy harvesting link based relay selection when increasing the number of relays. In Fig. 12, the system OP of MEDS scheme in case 1 outperforms that in case 2 since the system OP in case 2 is

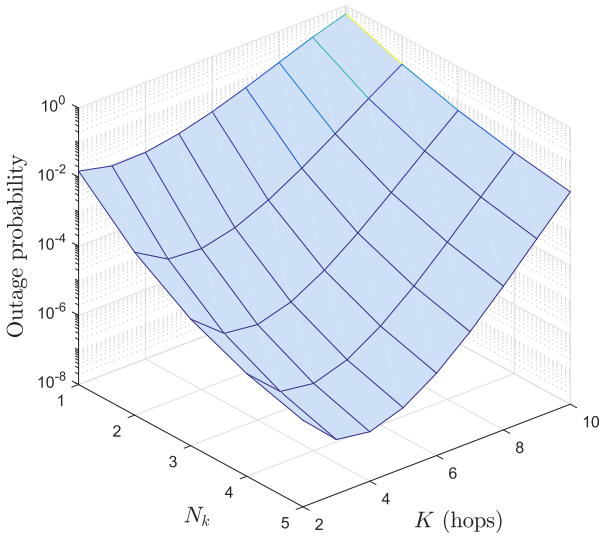

FIGURE 11. Effects of the number of hops and number of relays on the OP of MDS scheme with $\bar{\gamma} = -2$ dB, $M = 3$ and $L = 3$.

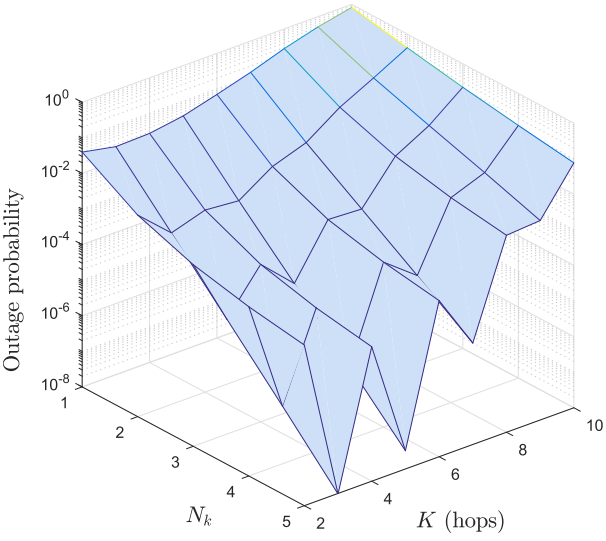

FIGURE 12. Effects of the number of hops and number of relays on the OP of MEDS scheme with $\bar{\gamma} = -2$ dB, $M = 3$ and $L = 3$.

dominated by the relay selection strategy employing in the first single hop transmission. Moreover, when increasing the number of hops remarkably increases the error probability for relaying signal to destination resulting in the system performance degradation of all schemes. In addition, for the same channel settings, the optimal number of hops, K_{opt}, takes the same value for RRS, MES, MDS schemes, e.g., $K_{\text{opt}} = 4$ while K_{opt} takes the value of 3 in MEDS scheme.

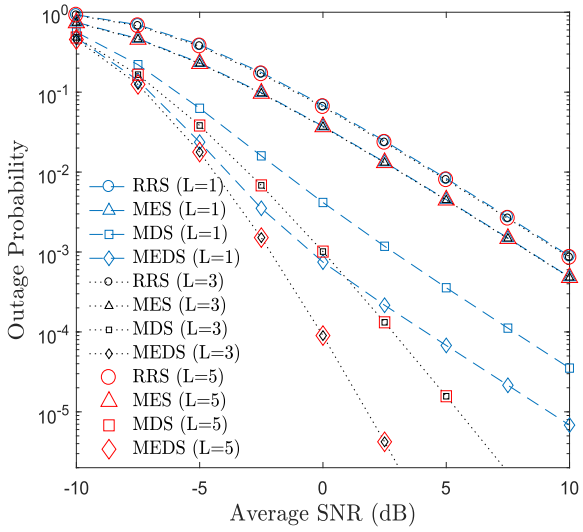

FIGURE 13. Effects of the destination's antennas on the system OP with $K = 7$, $N_k = 3$, $\bar{\gamma} = -2$ dB and $\alpha = 0.3$.

Fig. 13 shows the system OP as a function of the number of antennas at destination. For a given value of N_k, i.e., $N_k = 3$, we consider three cases of L, i.e., $L < N_k$, $L = N_k$ and $L > N_k$. As can be observed, the RRS and MES schemes give the same diversity gain in all three cases while the diversity gain of MEDS and MDS schemes increases in case of $L = N_k$ and $L > N_k$. This results reveal that adopting more receive antennas at D will achieve high diversity gain in multi-hop systems employing relay selection based on data channel link, i.e., MDS and MEDS schemes. Furthermore, when the number of antennas at D is greater than or equal to the number of relay in each cluster, the diversity gains of MEDS and MDS schemes are the same regardless of increasing number of antennas at D. This finding allows us to reduce the network complexity and achieve the best system performance.

V. CONCLUSIONS

In this paper, we have proposed the wireless powered cluster-based multi-hop relay schemes to improve the outage performance for cooperative multi-hop radio networks. In particular, we derive the exact closed-form expression of outage probability for the RRS, MES, MDS and MEDS schemes. The numerical results present that for the same channel configurations the MEDS scheme provides the best performance among those of MDS, MES and RRS schemes. Moreover, the system performance can be improved by increasing the number of PBs, growing the number of relays in each cluster, appropriately designing the time switching ratio for the energy process and number of hops for data transmission phase. As a result, it could be a promising scheme for wireless sensor networks to expand the network coverage and improve the network performance.

APPENDIX
PROOF OF THEOREM 1

The outage probability of RRS scheme can be rewritten as

$$\mathbb{P}_{out}^{\text{RRS}} = 1 - [1 - F_{\gamma_{\text{D}}^{\text{RRS}}}(\gamma_{\text{th}})] \prod_{k=1}^{K} [1 - F_{\gamma_{k,b,j}^{\text{RRS}}}(\gamma_{\text{th}})], \quad (80)$$

where $F_{\gamma_{\text{D}}^{\text{RRS}}}(.)$ and $F_{\gamma_{k,b,j}^{\text{RRS}}}(.)$ are the cumulative distribution function (CDF) of $\gamma_{\text{D}}^{\text{RRS}}$ and $\gamma_{k,b,j}^{\text{RRS}}$, respectively.

Let $X = \sum_{m=1}^{M} |g_{k-1,m,b}|^2$ and $Y = |h_{k,b,j}|^2$. The CDF of $\gamma_{k,b,j}^{\text{RRS}}$ can be calculated as

$$\begin{aligned} F_{\gamma_{k,b,j}^{\text{RRS}}}(\gamma_{\text{th}}) &= \Pr[\kappa \bar{\gamma} XY < \gamma_{\text{th}}] \\ &= \int_0^{+\infty} F_X\left(\frac{\gamma_{\text{th}}}{\kappa \bar{\gamma} x}\right) f_Y(x) dx, \end{aligned} \quad (81)$$

where $F_X(.)$ and $f_Y(.)$ denote the CDF and probability density function (PDF) of X and Y, respectively. Since X is the sum of M i.i.d. gamma distributed RVs, the CDF and PDF of X are given respectively as [16]

$$F_X(x) = 1 - \exp(-m_1 \Omega_{k-1} x) \sum_{t=0}^{m_1 M - 1} \frac{(m_1 \Omega_{k-1} x)^t}{t!}, \quad (82)$$

$$f_X(x) = \frac{(m_1 \Omega_{k-1})^{m_1 M} x^{m_1 M - 1}}{\Gamma(m_1 M)} \exp(-m_1 \Omega_{k-1} x), \quad (83)$$

where $\Gamma(z) = \int_0^{\infty} t^{z-1} e^{-t} dt$ denotes the Gamma function [28, eq. (6.1.1)].

Then, substituting the PDF of Y, i.e.,

$$f_Y(x) = \frac{(m_2 \lambda_k)^{m_2}}{\Gamma(m_2)} x^{m_2 - 1} \exp(-m_2 \lambda_k x), \quad (84)$$

and (82) into (81) and after some manipulations, we obtain $F_{\gamma_{k,b,j}^{\text{RRS}}}(\gamma_{\text{th}})$ as

$$\begin{aligned} &F_{\gamma_{k,b,j}^{\text{RRS}}}(\gamma_{\text{th}}) \\ &= 1 - \sum_{t=0}^{m_1 M - 1} \frac{1}{t!} \left(\frac{m_1 \Omega_{k-1} \gamma_{\text{th}}}{\kappa \bar{\gamma}}\right)^t \frac{(m_2 \lambda_k)^{m_2}}{\Gamma(m_2)} \\ &\quad \times \int_0^{+\infty} x^{m_2 - t - 1} \exp\left(-m_2 \lambda_k x - \frac{m_1 \Omega_{k-1} \gamma_{\text{th}}}{\kappa \bar{\gamma} x}\right) dx. \end{aligned} \quad (85)$$

With the help of [27, eq. (3.471.9)], the CDF of $\gamma_{k,b,j}^{\text{RRS}}$ can be obtained as

$$F_{\gamma_{k,b,j}^{\text{RRS}}}(\gamma_{\text{th}}) = 1 - \sum_{t=0}^{m_1 M-1} \frac{2}{t!\Gamma(m_2)} \left(\frac{m_1\Omega_{k-1}m_2\lambda_k\gamma_{\text{th}}}{\kappa\bar{\gamma}}\right)^{\frac{m_2+t}{2}} \times \mathbb{K}_{m_2-t}\left(2\sqrt{\frac{m_1\Omega_{k-1}m_2\lambda_k\gamma_{\text{th}}}{\kappa\bar{\gamma}}}\right). \quad (86)$$

In the last hop, by denoting $X_{\text{D}} = \sum_{m=1}^{M} |g_{K-1,m,b}|^2$ and $Z = \sum_{l=1}^{L} |h_{K,b,l}|^2$. The CDF of $\gamma_{\text{D}}^{\text{RRS}}$ can be calculated as

$$F_{\gamma_{\text{D}}^{\text{RRS}}}(\gamma_{\text{th}}) = \Pr[\kappa\bar{\gamma}X_{\text{D}}Z < \gamma_{\text{th}}] = \int_0^{+\infty} F_{X_{\text{D}}}\left(\frac{\gamma_{\text{th}}}{\kappa\bar{\gamma}x}\right) f_Z(x)dx. \quad (87)$$

Recalling that Z is the sum of L i.i.d. gamma RVs; thus, the PDF of Z can be expressed as

$$f_Z(x) = \frac{(m_2\lambda_K)^{m_2L}x^{m_2L-1}}{\Gamma(m_2L)}\exp(-m_2\lambda_K x). \quad (88)$$

Plugging the CDF of X_{D}, i.e.,

$$F_{X_{\text{D}}}(x) = 1 - \exp(-m_1\Omega_{K-1}x)\sum_{t=0}^{m_1M-1}\frac{(m_1\Omega_{K-1}x)^t}{t!}, \quad (89)$$

and (88) into (87) and then applying of [27, eq. (3.471.9)], we obtain as

$$F_{\gamma_{\text{D}}^{\text{RRS}}}(\gamma_{\text{th}}) = 1 - \sum_{t=0}^{m_1M-1}\frac{2}{t!}\left(\frac{m_1\Omega_{K-1}m_2\lambda_K\gamma_{\text{th}}}{\kappa\bar{\gamma}}\right)^{\frac{m_2L+t}{2}} \times \frac{1}{\Gamma(m_2L)}\mathbb{K}_{m_2L-t}\left(2\sqrt{\frac{m_1\Omega_{K-1}m_2\lambda_K\gamma_{\text{th}}}{\kappa\bar{\gamma}}}\right). \quad (90)$$

Having $F_{\gamma_{k,b,j}^{\text{RRS}}}(.)$ and $F_{\gamma_{\text{D}}^{\text{RRS}}}(.)$ at hands, plugging every things into (80), we obtain the desired result as (21), which also finish the proof here.

REFERENCES

[1] X. Lu, P. Wang, D. Niyato, D. I. Kim, and Z. Han, "Wireless networks with RF energy harvesting: A contemporary survey," *IEEE Commun. Surveys Tuts.*, vol. 17, no. 2, pp. 757–789, 2nd Quart., 2015.

[2] X. Zhou, R. Zhang, and C. K. Ho, "Wireless information and power transfer: Architecture design and rate-energy tradeoff," *IEEE Trans. Commun.*, vol. 61, no. 11, pp. 4754–4767, Nov. 2013.

[3] I. Krikidis, S. Timotheou, S. Nikolaou, G. Zheng, D. W. K. Ng, and R. Schober, "Simultaneous wireless information and power transfer in modern communication systems," *IEEE Commun. Mag.*, vol. 52, no. 11, pp. 104–110, Nov. 2014.

[4] R. Zhang and C. K. Ho, "MIMO broadcasting for simultaneous wireless information and power transfer," *IEEE Trans. Wireless Commun.*, vol. 12, no. 5, pp. 1989–2001, May 2013.

[5] A. A. Nasir, X. Zhou, S. Durrani, and R. A. Kennedy, "Relaying protocols for wireless energy harvesting and information processing," *IEEE Trans. Wireless Commun.*, vol. 12, no. 7, pp. 3622–3636, Jul. 2013.

[6] N. T. Van, H. M. Tan, T. M. Hoang, T. T. Duy, and V. N. Q. Bao, "Exact outage probability of energy harvesting incremental relaying networks with MRC receiver," in *Proc. IEEE Int. Conf. Adv. Technol. Commun.*, Hanoi, Vietnam, Oct. 2016, pp. 120–125.

[7] N. T. Do, V. N. Q. Bao, and B. An, "Outage performance analysis of relay selection schemes in wireless energy harvesting cooperative networks over non-identical Rayleigh fading channels," *Sensors*, vol. 16, no. 3, p. 295, Feb. 2016.

[8] N. T. Do, D. B. da Costa, T. Q. Duong, V. N. Q. Bao, and B. An, "Exploiting direct links in multiuser multirelay SWIPT cooperative networks with opportunistic scheduling," *IEEE Trans. Wireless Commun.*, vol. 16, no. 8, pp. 5410–5427, Aug. 2017.

[9] C. Zhong, X. Chen, Z. Zhang, and G. K. Karagiannidis, "Wireless-powered communications: Performance analysis and optimization," *IEEE Trans. Commun.*, vol. 63, no. 12, pp. 5178–5190, Oct. 2015.

[10] M. Xia and S. Aissa, "On the efficiency of far-field wireless power transfer," *IEEE Trans. Signal Process.*, vol. 63, no. 11, pp. 2835–2847, Jun. 2015.

[11] Y. Liu, S. A. Mousavifar, Y. Deng, C. Leung, and M. Elkashlan, "Wireless energy harvesting in a cognitive relay network," *IEEE Trans. Wireless Commun.*, vol. 15, no. 4, pp. 2498–2508, Apr. 2016.

[12] K. Huang and V. K. N. Lau, "Enabling wireless power transfer in cellular networks: Architecture, modeling and deployment," *IEEE Trans. Wireless Commun.*, vol. 13, no. 2, pp. 902–912, Feb. 2014.

[13] H. Ju and R. Zhang, "Throughput maximization in wireless powered communication networks," *IEEE Trans. Wireless Commun.*, vol. 13, no. 1, pp. 418–428, Jan. 2014.

[14] H. Chen, Y. Li, J. L. Rebelatto, B. F. Uchoa-Filho, and B. Vucetic, "Harvest-then-cooperate: Wireless-powered cooperative communications," *IEEE Trans. Signal Process.*, vol. 63, no. 7, pp. 1700–1711, Apr. 2015.

[15] T. Q. Duong, V. N. Q. Bao, and H. J. Zepernick, "On the performance of selection decode-and-forward relay networks over Nakagami-*m* fading channels," *IEEE Commun. Lett.*, vol. 13, no. 3, pp. 172–174, Mar. 2009.

[16] Z. Chen, Z. Chi, Y. Li, and B. Vucetic, "Error performance of maximal-ratio combining with transmit antenna selection in flat Nakagami-*m* fading channels," *IEEE Trans. Wireless Commun.*, vol. 8, no. 1, pp. 424–431, Jan. 2009.

[17] P. V. T. Anh, V. N. Q. Bao, and N. K. Le, "On the performance of wireless energy harvesting TAS/MRC relaying networks over Nakagami-*m* fading channels," in *Proc. 3rd Nat. Found. Sci. Technol. Develop. Conf. Inf. Comput. Sci.*, Danang, Vietnam, Sep. 2016, pp. 1–5.

[18] N. P. Le, "Throughput analysis of power-beacon assisted energy harvesting wireless systems over non-identical Nakagami-*m* fading channels," *IEEE Commun. Lett.*, to be published, doi: 10.1109/LCOMM.2017.2756053.

[19] O. O. Ogundile and A. S. Alfa, "A survey on an energy-efficient and energy-balanced routing protocol for wireless sensor networks," *Sensors*, vol. 17, no. 5, p. 1084, May 2017.

[20] T. T. Duy and H. Y. Kong, "Secrecy performance analysis of multihop transmission protocols in cluster networks," *Wireless Pers. Commun.*, vol. 82, no. 4, pp. 2505–2518, Feb. 2015.

[21] V. N. Q. Bao and T. Q. Duong, "Outage analysis of cognitive multihop networks under interference constraints," *IEICE Trans. Commun.*, vol. E95-B, no. 3, pp. 1019–1022, Mar. 2012.

[22] V. N. Q. Bao, T. Q. Duong, and C. Tellambura, "On the performance of cognitive underlay multihop networks with imperfect channel state information," *IEEE Trans. Commun.*, vol. 61, no. 12, pp. 4864–4873, Dec. 2013.

[23] S. Q. Nguyen and H. Y. Kong, "Exact outage analysis of the effect of co-channel interference on secured multi-hop relaying networks," *Int. J. Electron.*, vol. 103, no. 11, pp. 1822–1838, Mar. 2016.

[24] F. S. Al-Qahtani, R. M. Radaydeh, S. Hessien, T. Q. Duong, and H. Alnuweiri, "Underlay cognitive multihop MIMO networks with and without receive interference cancellation," *IEEE Trans. Commun.*, vol. 65, no. 4, pp. 1477–1493, Apr. 2017.

[25] C. Xu, M. Zheng, W. Liang, H. Yu, and Y.-C. Liang, "Outage performance of underlay multihop cognitive relay networks with energy harvesting," *IEEE Commun. Lett.*, vol. 20, no. 6, pp. 1148–1151, Jun. 2016.

[26] E. Chen, M. Xia, D. B. da Costa, and S. Aïssa, "Multi-hop cooperative relaying with energy harvesting from cochannel interferences," *IEEE Commun. Lett.*, vol. 21, no. 5, pp. 1199–1202, May 2017.

[27] I. S. Gradshteyn and I. M. Ryzhik, *Table of Integrals, Series, and Products*. San Diego, CA, USA: Academic, 2007.

[28] M. Abramowitz and A. I. Stegun, *Handbook of Mathematical Functions With Formulas, Graphs, and Mathematical Tables*, vol. 9. New York, NY, USA: Dover, 1972.

[29] A. Papoulis and S. U. Pillai, *Probability, Random Variables, and Stochastic Processes*, 4th ed. New York, NY, USA: McGraw-Hill, 2002.

NGUYEN TOAN VAN received the B.S. degree in electronics and telecommunications engineering and the M.S. degree in electronics engineering from the Ho Chi Minh City University of Technology and Education, Vietnam, in 2011 and 2014, respectively. He is currently pursuing the Ph.D. degree in electronics and computer engineering with Hongik University. His main research topics are wireless communications, energy harvesting, and cooperative and cognitive communications.

TRI NHU DO (S'16) was born in Da Nang, Vietnam. He received the B.S. degree in electronics and telecommunications engineering from the Posts and Telecommunications Institute of Technology, Vietnam, in 2012, and the M.S. degree in electronics and computer engineering from Hongik University, Sejong City, South Korea, in 2015, where he is currently pursuing the Ph.D. degree in electronics and computer engineering. He is also a Teaching Associate in electronics and computer engineering with Hongik University. His main research topics are wireless communications and cooperative relaying transmissions.

VO NGUYEN QUOC BAO (M'11–SM'16) served as the Dean of the Faculty of Telecommunications and the Director of the Wireless Communication Laboratory. He is currently an Associate Professor of wireless communications with the Posts and Telecommunications Institute of Technology, Vietnam. He has authored over 140 journal and conference articles that have over 1500 citations and H-index of 21. His research interests include wireless communications and information theory with current emphasis on MIMO systems, cooperative and cognitive communications, physical layer security, and energy harvesting. He is a member of the Executive Board of the Radio-Electronics Association of Vietnam and the Electronics Information and Communications Association Ho Chi Minh City. He served as the Technical Program Co-Chair of ATC (2013 and 2014), NAFOSTED, NICS (2014, 2015, and 2016), REV-ECIT 2015, ComManTel (2014 and 2015), and SigTelCom 2017. He is currently serving as a Scientific Secretary of the Vietnam National Foundation for Science and Technology Development Scientific Committee in Information Technology and Computer Science. He is an Associate Editor of the *EURASIP Journal on Wireless Communications and Networking*, an Editor of the *Transactions on Emerging Telecommunications Technologies* (Wiley ETT), the *VNU Journal of Computer Science and Communication Engineering*, and the *REV Journal on Electronics and Communications*.

BEONGKU AN received the B.S. degree in electronic engineering from Kyungpook National University, South Korea, in 1988, the M.S. degree in electrical engineering from the New York University (Polytechnic), Brooklyn, NY, USA, in 1996, and the Ph.D. degree from the New Jersey Institute of Technology (NJIT), Newark, NJ, USA, in 2002. From 1989 to 1993, he was a Senior Researcher with RIST, Pohang, South Korea. He was a Lecturer and an RA with NJIT from 1997 to 2002. He joined the Faculty of the Department of Computer and Information Communications Engineering, Hongik University, South Korea, where he is currently a Professor. His current research interests include mobile wireless networks and communications, such as ad-hoc networks, sensor networks, wireless internet, cognitive radio networks, ubiquitous networks, cellular networks, IoT, cooperative routing, multicast routing, energy harvesting, physical layer security, visible light communication, cross-layer technology, and mobile cloud computing. He was listed in Marquis *Who's Who in Science and Engineering* and Marquis *Who's Who in the World*. He was the President of the Institute of Electronics and Information Engineers, Computer Society, in 2012. Since 2013, he has been a General Chair of the International Conference on Green and Human Information Technology.